CE-NAS: An End-to-End Carbon-Efficient Neural Architecture Search Framework

Yiyang Zhao
Worcester Polytechnic Institute

Yunzhuo Liu
Shanghai Jiao Tong University

Bo Jiang
Shanghai Jiao Tong University

Tian Guo
Worcester Polytechnic Institute

Abstract

This work presents a novel approach to neural architecture search (NAS) that aims to increase carbon efficiency for the model design process. The proposed framework CE-NAS addresses the key challenge of high carbon cost associated with NAS by exploring the carbon emission variations of energy and energy differences of different NAS algorithms. At the high level, CE-NAS leverages a reinforcement-learning agent to dynamically adjust GPU resources based on carbon intensity, predicted by a time-series transformer, to balance energy-efficient sampling and energy-intensive evaluation tasks. Furthermore, CE-NAS leverages a recently proposed multi-objective optimizer to effectively reduce the NAS search space. We demonstrate the efficacy of CE-NAS in lowering carbon emissions while achieving SOTA results for both NAS benchmarks and open-domain NAS tasks. For example, on the HW-NasBench, CE-NAS reduces carbon emissions by up to 7.22X while maintaining a search efficiency comparable to vanilla NAS. For open-domain NAS tasks, CE-NAS achieves SOTA results with 97.35% top-1 accuracy on CIFAR-10 with only 1.68M parameters and a carbon consumption of 38.53 lbs of CO_2. On ImageNet, our searched model achieves 80.6% top-1 accuracy with a 0.78 ms TensorRT latency using FP16 on NVIDIA V100, consuming only 909.86 lbs of CO_2, making it comparable to other one-shot-based NAS baselines. Our code is available at https://github.com/cake-lab/CE-NAS.

1 Introduction

Deep Learning (DL) has become an increasingly important field in computer science, with wide applications such as healthcare and finance [81, 6, 60, 30, 33, 63, 35, 38]. Neural architecture search (NAS) has emerged as a means to automate the design of DL models, which involves training *many DL models* from a massive architecture design space with hundreds of millions to trillions of candidates [102, 66, 79, 97, 98, 46]. Consequently, NAS can be energy-intensive and significantly contributes to today's carbon emissions [68, 102]. Many NAS works have reported using thousands of GPU-hours [102, 66, 79, 78, 98]. For example, Zoph et al. [102] used 800 GPUs for 28 days, resulting in 22,400 GPU-hours, to obtain the final architectures. Strubell et al. [68] found that a single NAS solution can emit as much carbon as five cars during its lifetime.

The environmental impact of NAS, if left untamed, can be substantial. While recent works have significantly improved the search efficiency of NAS [102, 66, 79, 78, 97], e.g., reducing the GPU-hours to tens of hours without sacrificing the architecture quality, there still lacks *conscious efforts in reducing carbon emissions*. As noted in a recent vision paper by Bashir et al. [9], energy efficiency can help reduce carbon emissions but is not equivalent to carbon efficiency. This paper aims to

38th Conference on Neural Information Processing Systems (NeurIPS 2024).

https://doi.org/10.52202/079017-2628

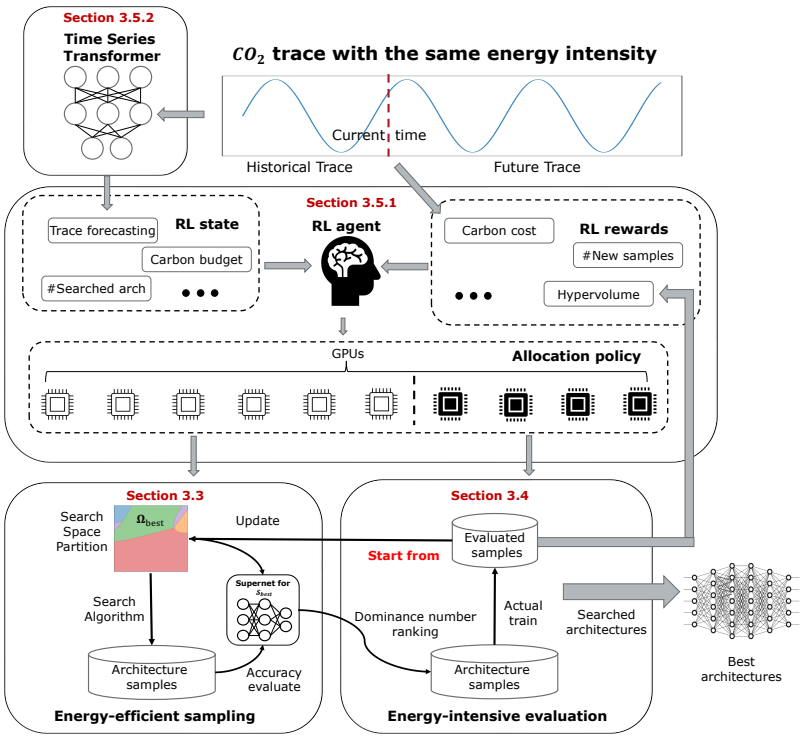

Figure 1: An overview of CE-NAS. The sampling and evaluation tasks will be allocated different GPU resources based on carbon emission intensity during the neural architecture search. Specifically, when the CO_2 intensity is low, we allocate more resources to energy-intensive evaluation, which focuses on assessing the performance of sampled architectures generated through energy-efficient sampling. Conversely, when CO_2 intensity is high, more GPUs are dedicated to energy-efficient sampling, which utilizes various NAS algorithms to sample new architectures from a search space partitioned based on previously evaluated architectures. The specific GPU allocation strategy is learned through a reinforcement learning agent, as detailed in the middle section of the figure.

bridge the gap between carbon and energy efficiency with a new NAS framework designed to be carbon-aware from the outset.

The proposed framework, termed CE-NAS, tackles the high carbon emission problem from two main aspects. First, CE-NAS regulates the model design process by *deciding when to use different NAS evaluation strategies based on the carbon intensity*, which varies geographically and temporally with the mix of active generators as observed in [9]. To elaborate, given a fixed amount of GPU resources, CE-NAS will allocate more resources to energy-efficient NAS evaluation strategies, e.g., one-shot NAS [65, 10, 46, 97, 14, 13], during periods of high carbon intensity. Conversely, during periods of low carbon intensity, CE-NAS will shift the focus to running energy-intensive but more effective NAS evaluation strategies, e.g., vanilla NAS [102, 66, 79, 78]. We design and train a reinforcement learning (RL) agent (§3.5) based on historical and predicted carbon emissions (§3.5.2) and observed search results to make such allocation decisions. Second, the CE-NAS framework will support searching for DL models satisfying multiple metrics beyond the commonly used metric of inference accuracy. CE-NAS can consider more metrics such as inference latency, #PARAMs, #FLOPs, etc. For example, CE-NAS can search for models with high accuracy and low inference latency. Specifically, both the search and deployment efficiency are achieved by integrating a recent learning-based multi-objective optimizer LaMOO [98] to CE-NAS. Figure 1 depicts the overall workflow of CE-NAS.

To demonstrate CE-NAS's efficacy in addressing the energy and carbon issues, we conduct a comprehensive evaluation using both commonly used NAS benchmarks and real-world NAS tasks. For example, utilizing carbon emission data from ElectricityMap [58], CE-NAS achieves better performance with reduced carbon costs compared to existing methods on various NAS benchmarks, including HW-NASBench [40] and NasBench301 [93]. In open-domain tasks, CE-NAS achieves the state-of-the-art (SOTA) top-1 accuracy of 97.35% with only 1.68M parameters on the CIFAR-10

image classification task, with CO_2 costs similar to those of one-shot-based NAS algorithms. For the ImageNet dataset, CE-NAS achieves the SOTA top-1 accuracy of 80.6% under the same inference latency of 0.78 ms with TensorRT on NVIDIA V100, while maintaining a carbon cost comparable to SOTA NAS methods [13]. We also evaluate our carbon forecasting model and show that it outperforms existing models [11, 56, 55], including the SOTA method [55].

In summary, we make the following key contributions.

- We introduce a carbon-efficient NAS framework named CE-NAS that can dynamically allocate GPU resources among different NAS evaluation methods—namely, vanilla NAS and one/few-shot NAS—based on carbon emissions data and current search results. CE-NAS is an end-to-end framework that synergistically integrates an RL-based agent for GPU resource allocation, a time-series transformer [2] for carbon intensity prediction, and a multi-objective optimizer [98] for reduced search space.
- We implement and evaluate CE-NAS on different NAS benchmarks, including HW-NasBench [40] and Nasbench301 [93]. We show that CE-NAS can achieve the best search performance compared to only using vanilla NAS, one-shot NAS, and a recently proposed heuristic GPU allocation strategy [4] given the same carbon budget.
- CE-NAS delivers SOTA architectural performance in open-domain NAS tasks while maintaining carbon costs comparable to one-shot NAS methods. For example, on CIFAR-10, CE-NAS achieves a top-1 accuracy of 97.35% with only 1.68M parameters and a carbon cost of 38.53 lbs CO_2. On ImageNet, CE-NAS reaches a top-1 accuracy of 80.6% with a 0.78 ms TensorRT latency using FP16 on NVIDIA V100.

2 Related Work

Efficient neural architecture search (NAS) often focuses on improving the evaluation phase, e.g., via weight-sharing (one-shot) [65, 46, 88, 18, 13], zero-shot proxy [41, 85, 3, 37, 73, 76, 95, 74, 50, 59, 44, 70, 16, 17], performance predictor [45, 13, 79, 93], low-fidelity NAS evaluation [102, 66, 79, 78, 46, 36], and gradient proxy NAS [87]. A comparison of these methods can be found in Table 4 in Appendix. Weight-sharing leverages the accuracy estimated by a *supernet* as a proxy for the true architecture performance, while gradient proxy NAS uses the gradient as a proxy. These proxy-based methods, although incurring smaller search costs in terms of energy, can have lower search efficiency because their estimated architecture accuracy may have poor rank correlation [97]. Zero-shot proxy NAS eliminates the need for *supernet* training entirely, serving as a fully training-free proxy for network evaluation. However, as noted in [41], mainstream zero-shot NAS methods still struggle to achieve high rank correlations between predicted and true accuracies, even when compared to weight-sharing-based NAS evaluation. Performance predictors provide a more accurate performance prediction than weight-sharing and gradient proxy NAS. Still, their accuracy heavily relies on the volume and quality of the training data, which can be very expensive to create [90, 93]. Low-fidelity evaluation still requires training each searched architecture, leading to limited energy savings. In practice, simply employing these methods without modification might not effectively balance carbon emissions and performance during the search process. CE-NAS successfully achieves good search efficiency, search quality, and carbon efficiency by integrating the weight-sharing NAS method into vanilla NAS. We also leverage the low-fidelity evaluation method in the open-domain NAS search.

The high carbon emission of NAS is a pressing issue. A study by [68] found that a single NAS solution can emit as much carbon as five cars over its lifetime. For example, if we design a transformer-based model, training a base Transformer model can use 96 GPU hours on NVIDIA's P100 [68], while training a larger model can take 28 GPU days. A recent NAS work [68] on transformer revealed that their comprehensive architecture search used 979 million training steps, totaling 274,120 GPU hours and resulting in 626,155 pounds of CO_2 emissions. Although several NAS studies [87, 13, 12] have attempted to address carbon issues during the search process, they often treat carbon emissions uniformly, regardless of time and location variances. These carbon-agnostic NAS methods therefore miss the opportunity to explore the inherent carbon variations [9]. Concurrently, systems researchers have explored the temporal and spatial variations exhibited in electricity's carbon emission for popular data center applications like training [4, 9] and inference [39]. This work targets a special form of training workload, i.e., NAS, by leveraging the domain knowledge to optimize the end-to-end NAS process to explore carbon variations. Specifically, we concentrate on implementing the temporal

 https://doi.org/10.52202/079017-2628

variations in carbon intensity rather than spatial variations, as managing the carbon costs associated with spatial shifts poses significant challenges. Transferring large volumes of data over the Internet can incur substantial carbon costs, and accurately estimating these costs is complex. Data often passes through numerous intermediate routers across large geographic regions, making it difficult to ensure that the benefits of a spatial shift outweigh its associated overhead.

3 The Design of a Carbon-Efficient NAS Framework

In this section, we present an overview of the proposed CE-NAS framework (§3.1). We first introduce the initial setup of our CE-NAS in §3.2. We then propose a sampling strategy based on the one-shot/few-shot NAS evaluation method in §3.3. Finally, we discuss the architecture evaluation part in §3.4, which is both time and computing resource-intensive. In §3.5, we describe how to use an RL-based agent to automatically allocate GPU resources based on predicted hourly carbon intensity.

3.1 CE-NAS Overview

As observed in [9], grid carbon emissions vary geographically and temporally based on the mix of active generators. Consequently, systems can emit different amounts of carbon even when consuming the same electricity at different locations or times. Currently, neither one (few)-shot nor vanilla NAS methods account for these variations in carbon emissions, which can lead to inefficiencies in terms of NAS carbon usage. Furthermore, one (few)-shot and vanilla NAS exhibit different search and carbon efficiency trade-offs. Vanilla NAS is carbon-intensive but effective, while one (few)-shot NAS can be carbon-friendly but sample-inefficient.

CE-NAS is a NAS framework that directly addresses the high-carbon issues by balancing energy consumption across high-carbon and low-carbon periods. The primary objective of this framework is to efficiently search for optimal neural architectures while minimizing the carbon footprint associated with the NAS process. Specifically, CE-NAS decouples the two parts of a NAS search process—energy-efficient sampling and energy-intensive evaluation—and handles them independently across different carbon periods. For each carbon period, CE-NAS uses an RL-based agent to automatically allocate GPU resources for the NAS search process to achieve good carbon efficiency.

3.2 Search Initialization

CE-NAS considers more than one search objective(e.g., accuracy, mAP, latency, #FLops, etc), so we formulate the search problem as a multi-objective optimization (MOO). Similar to other NAS and optimization problems [24, 77, 98, 66], CE-NAS initializes the search process by randomly selecting several architectures, $\mathbf{a}$, from the search space, Ω, and evaluating their accuracy, $E(\mathbf{a})$, and other deployment metrics (#Params, #FLops, inference latency, inference energy, etc) $T(\mathbf{a})$. Compared to the accuracy $E(\mathbf{a})$, $T(\mathbf{a})$ can be quickly measured without much cost. The resulting samples are then added to the observed samples set, $\mathcal{P}$.

We distinguish two types of methods for evaluating the accuracy of an architecture. One is actual training, which trains an architecture a from scratch until convergence and evaluates it to obtain its true accuracy, $E(a)$. To optimize computing resources during this process, we implement the low-fidelity training strategy described in [102, 66, 46, 79, 36]. This strategy reduces computing costs by simplifying the parameters of neural architectures (e.g., #depth, #channels, #resolutions) or shortening the training process under controlled conditions. The other method is using *one-shot evaluation* [10, 65, 46], which leverages a trained *supernet*, or a zero-shot-based NAS evaluator [95, 74, 50, 59, 44, 70, 16, 17] as a performance proxy to estimate the accuracy of the architecture, denoted as $E'(a)$. Note that obtaining $E'(a)$ is very cheap and carbon-efficient; however, due to the co-adaption among operations [97], $E'(a)$ is often not as accurate as $E(a)$. We train all the sampled architectures in the initialization stage to obtain their true accuracy for further search.

3.3 Energy-Efficient Architecture Sampling

Multi-objective search space partition. We leverage the recently proposed multi-objective optimizer called LaMOO [98] that learns to partition the search space from observed samples to focus on

promising regions likely to contain the Pareto frontier. LaMOO is an optimizer for general black-box optimization problems; we can apply it to NAS as follows.

We utilize LaMOO [98] to partition the search space Ω into several subspaces, and find the optimal subspace denoted by Ω_{best}. Next, we construct and train a supernet [10, 97], $\mathcal{S}_{best}$, for Ω_{best}. We then use a NAS search algorithm to identify new architectures that will be used to refine the search space. In this work, we employ the state-of-the-art multi-objective Bayesian optimization algorithm qNEHVI [25]. This algorithm will generate new architectures $\boldsymbol{a_n}$ from Ω_{best}, and estimate their approximate accuracy $E'(\boldsymbol{a_n})$ using $\mathcal{S}_{best}$. At the same time, these architectures $\boldsymbol{a_n}$ are added to a ready-to-train set $\mathcal{R}$, consisting of candidates for further actual training as described in §3.4.

We define the maximum capacity of $\mathcal{R}$ as $Cap(\mathcal{R})$, hyperparameter in `CE-NAS`. Note that the architectures in $\mathcal{R}$ are removed once they are actual trained as described in §3.4. When the capacity is reached, i.e., when there are more architectures to train than we have resources for, the sampling process blocks until spaces free up in $\mathcal{R}$. The accuracy of architectures estimated by $\mathcal{S}_{best}$ will be fed back into the search algorithm as shown in Figure 1 to repeat the process described above.

As mentioned in §3.2, obtaining estimated accuracy through supernet is energy-efficient because these architectures can be evaluated without the time-consuming training. Therefore, during high carbon emission periods, `CE-NAS` will try to perform this process to save energy and produce as little carbon as possible, as shown in the *energy-efficient sampling* part of Fig.1.

3.4 Energy-Intensive Architecture Evaluation

If we perform the entire NAS only using the process described in §3.3, `CE-NAS` will be essentially performing one/few-shot NAS only within the subspace $\mathcal{S}_{best}$. Although these methods are efficient, they typically underperform compared to vanilla NAS. As Zhao et al. showed, it is possible to improve LaMOO's space partition with more observed samples through actual training [98]. This section describes the process to evolve $\mathcal{S}_{best}$ during low carbon emission periods.

At the high level, we will pick new architectures from the ready-to-train set $\mathcal{R}$ to train to convergence and use them to refine the search space partition. That is, the architecture $\boldsymbol{a}$, with its true accuracy, $E(\boldsymbol{a})$, will be added to the observed sample set $\mathcal{P}$ to help identify a more advantageous subspace, Ω_{best}, for the architecture sampling process as described in [98]. In this work, we sort the architectures in the ready-to-train set $\mathcal{R}$ by their *dominance number*. The dominance number $o(\boldsymbol{a})$ of an architecture $\boldsymbol{a}$ is defined as the number of samples that dominate $\boldsymbol{a}$ in search space Ω:

$$o(\boldsymbol{a}) := \sum_{\boldsymbol{a}_i \in \Omega} \mathbb{I}[\boldsymbol{a}_i \prec_f \boldsymbol{a},\ \boldsymbol{a} \neq \boldsymbol{a}_i]^1, \tag{1}$$

where $\mathbb{I}[\cdot]$ is the indicator function. With the decreasing of the $o(\boldsymbol{a})$, $\boldsymbol{a}$ would be approaching the Pareto frontier; $o(\boldsymbol{a}) = 0$ when the sample architecture $\boldsymbol{a}$ is located in the Pareto frontier. The use of dominance number allows us to rank an architecture by considering both the estimated accuracy $E'(\boldsymbol{a})$ and other metrics $T(\boldsymbol{a})$ at the same time. `CE-NAS` will first train the architectures with lower dominance number values when GPU resources are available. Once an architecture is trained, it is removed from $\mathcal{R}$.

This process is depicted in the *energy-consuming evaluation* component of Figure 1. Note that this process includes actual time-consuming DL model training, which is time-consuming and highly energy-intensive, leading to significant CO_2 emissions. Hence, `CE-NAS` will try to prioritize this process during periods of low carbon intensity.

3.5 Carbon-Efficient GPU Allocation

The carbon impact of the above two processes (i.e., §3.3 and §3.4) in a NAS search is materialized through the use of GPU resources. A key decision `CE-NAS` needs to make is *how* to allocate GPUs among these two interdependent processes. Assigning too many GPUs to architecture sampling could impact the search efficiency, i.e., the searched architectures are far from the true Pareto frontier; assigning too many GPUs to architecture evaluation could significantly increase energy consumption and carbon emission. `CE-NAS` must consider these trade-offs under varying carbon intensity and

[1]We define *dominance* $\boldsymbol{y} \prec_f \boldsymbol{x}$ as $f_i(\boldsymbol{x}) \leq f_i(\boldsymbol{y})$ for all functions f_i, and exists at least one i s.t. $f_i(\boldsymbol{x}) < f_i(\boldsymbol{y})$, $1 \leq i \leq M$, where M is the number of objectives.

https://doi.org/10.52202/079017-2628

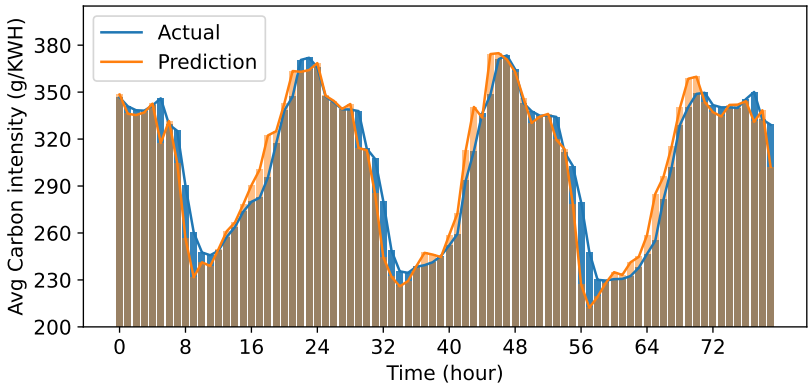

Figure 2: An overview of CE-NAS. This carbon trace is based on the US-CAL-CISO data from 2021, specifically covering the period from 0:00, July 2, 2021, to 8:00, July 4, 2021. The blue trace is its actual carbon trace and the yellow trace is the prediction trace by our carbon predictor described in sec. 3.5.2

re-evaluate the GPU allocation strategy. We design an RL-based strategy (§3.5.1) to automatically allocate GPU resources based on predicted carbon intensity in every one hour (§3.5.2).

3.5.1 Design of RL-Based GPU Allocation Strategy

Although the heuristic-based strategy proposed by [4] can adjust the tendency for sampling and evaluation based on carbon intensity, it is still far from making the most carbon-efficient decision. It overlooks critical influencing factors such as the varying gains in accuracy from performing sampling and evaluation at different stages of the search. These factors are specific to the NAS algorithms and are challenging to model, which complicates its inclusion in heuristic strategy design. To address this issue, we introduce a method based on reinforcement learning that automatically accounts for these diverse factors to develop allocation strategies. We propose a Reinforcement Learning (RL)-based method to automatically customize a GPU allocation strategy for specific NAS algorithms. In this paper, we choose LaMOO [98] with qNEHVI [25].

The key to applying RL lies in the design of effective state inputs, actions, and rewards according to the specific task. Our CE-NAS focuses on tailoring these elements for carbon-efficient NAS tasks, with the guiding principle of simplifying the state and action spaces to expedite efficient and rapid training. Specifically, Our RL agent, which is a simple-structured neural network with only four fully connected layers, takes the remaining carbon budget, the number of already searched architectures and their hypervolume (The definition of the hypervolume refers to Appendix E.2.4.), as well as the future carbon traces predicted by the time transformer as input. Then it outputs the probabilities of different GPU allocation ratios for architecture evaluation as action. These possible allocation ratios are discretized to boost learning efficiency. After the action is executed, CE-NAS generates a reward based on the improvement of the performance of the already searched architectures and then uses the reward to refine the policies of the agent by updating its network parameters with the *actor-critic* [61] policy gradient algorithm. The specifics of our RL design can be found in Appendix C and the middle part of Fig. 1.

3.5.2 Design of Transformer-Based Carbon Intensity Forecasting

We utilize a machine learning model to predict future carbon intensity, which serves as the input of the RL agent. We leverage a time series transformer-based model, as shown in the top left part of Fig. 1, to forecast future carbon intensity because of their efficacy [62, 84, 99]. Specifically, we leverage the architecture design by employing a standard encoder-decoder Transformer for time series forecasting [2]. This method incorporates temporal features that act as positional encodings within the Transformer's encoder/decoder framework. Past values are input into the encoders, and future values are input into the decoders in the training stage. For instance, as described in [2], if a time series data point corresponds to the 11th of August, the temporal feature vector would be (11, 8), where 11 denotes the day of the month, and 8 signifies the month of the year. We leverage the SOTA

Table 1: Daywise MAPE comparison of our time-series transformer and other baseline methods.

Region	Day-1 Forecast				Day-2 Forecast				Day-3 Forecast			
	STCF [11]	DACF [56]	CC [55]	ours	STCF [11]	DACF [56]	CC [55]	ours	STCF [11]	DACF [56]	CC [55]	ours
CISO	10.71	6.45	8.08	**5.26**	18.99	12.26	11.19	**8.69**	25.24	16.02	12.93	**10.83**
DE	15.54	7.21	7.81	**5.34**	31.56	11.82	10.69	**8.23**	42.16	13.95	12.80	**10.68**
PJM	4.27	3.08	3.69	**2.58**	7.11	5.51	4.93	**3.53**	8.90	7.06	5.87	**4.02**

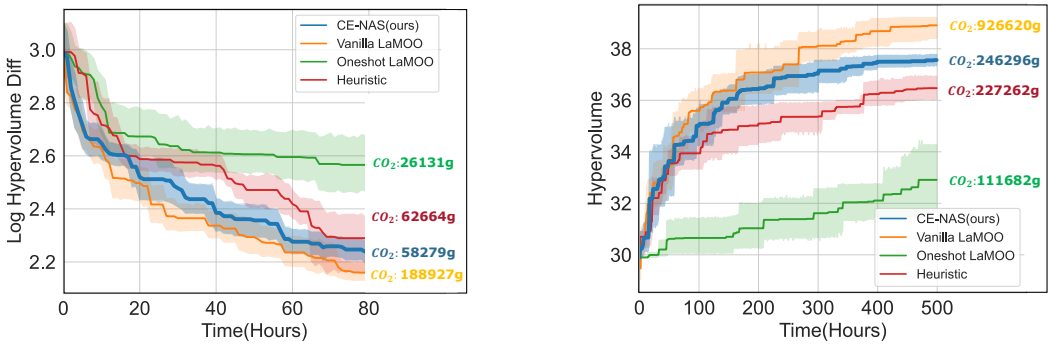

(a) HW-NAS-Bench (b) NasBench301

Figure 3: Search progress over time. CE-NAS has the second lowest relative carbon emission while achieving the second best $HV_{\text{log\_diff}}$ on HW-NAS-Bench, and CE-NAS has the second lowest relative carbon emission while achieving the second best HV on NasBench301.

NAS algorithm LaMOO [98] to design the architecture of the time series transformer. The details of search space and founded architectures are in Appendix D.

4 CE-NAS Experimental Evaluation

We develop a prototype of the CE-NAS framework as outlined in Section 3. This section analyzes CE-NAS's carbon efficiency and search efficacy through trace-driven simulations and emulation. We first demonstrate the performance of our designed time-series transformer for carbon forecasting in § 4.1. We then assess CE-NAS across two distinct NAS scenarios: the first leveraging two commonly used NAS benchmarks, HW-NAS-Bench [40] and NasBench301 [93], and the second including real-world computer vision applications, such as image classification.

Our experiments utilize carbon trace data sourced from ElectricityMap [58], an independent carbon information service. We selected the CISO[2] trace beginning on July 2, 2021, due to its variable carbon intensity, which provides an opportunity to evaluate CE-NAS's performance over time and its adaptability to fluctuating carbon levels. Figure 2 illustrates the initial 80 hours of the carbon trace, demonstrating the actual data against the forecasted trace predicted by our designed time series transformer, as detailed in Section 3.5.2. Throughout the CE-NAS search phase, predicted carbon intensity is utilized for GPU allocation, while the actual carbon trace informs the calculation of carbon costs in the evaluation phase.

We also conduct several ablation studies detailed in Appendix F. These studies include variations of hyperparameters in the RL agent settings, validation of LaMOO's effectiveness, and a comparison of search performance using predicted versus actual carbon traces, among others. Our findings reveal only a minimal difference in search performance between using predicted and actual carbon traces.

4.1 Time-series Transformer for Carbon Forcasting

We assess the performance of our time series forecasting transformer across three distinct regions: CISO, DE[3], and PJM[4]. We compare our approach against other SOTA models referenced in [11, 56,

[2]CISO: California Independent System Operator
[3]DE: Germany
[4]PJM: Pennsylvania-Jersey-Maryland Interconnection

https://doi.org/10.52202/079017-2628

Table 2: Search Results on CIFAR-10 using the NasNet search space. The two optimization objectives we are searching for are #params and accuracy.

Method	Test Error(%)	#Param (M)	Search&Training Cost (GPU Hours)†	CO_2 (lbs)	NAS Method
PNAS [45]	3.41±0.09	3.2	5400	3836.62	vanilla
NAO [54]	3.14±0.09	3.2	5400	3836.62	vanilla
NASNet-A [102]	2.65	3.3	48000	30534.78	vanilla
LEMONADE [29]	2.58	13.1	2160	1514.07	vanilla
AlphaX [79]	2.54±0.06	2.83	24000	16196.72	vanilla
AmoebaNet-B-small [66]	2.50±0.05	2.8	75600	43972.18	vanilla
BayeNAS [100]	2.81±0.04	3.4	31.2	21.70	one-shot
DARTS [46]	2.76±0.09	3.3	50.4	34.04	one-shot
MergeNAS [80]	2.68±0.01	2.9	40.8	27.01	one-shot
One-shot REA	2.68±0.03	3.5	44.4	29.33	one-shot
CNAS [43]	2.60±0.06	3.7	33.6	23.19	one-shot
PC-DARTS [88]	2.57±0.07	3.6	33.6	23.19	one-shot
Fair-DARTS [21]	2.54±0.05	3.32	98.4	65.87	one-shot
P-DARTS [18]	2.50	3.4	33.6	23.19	one-shot
CE-Net-P1	2.65±0.03	**1.68**	228.6	38.53	hybrid
CE-Net-P2	**2.16±0.06**	3.30	228.6	38.53	hybrid

† The total cost includes both the NAS search duration and the training time for the architectures identified. When applying one-shot NAS to search architectures on CIFAR-10, we estimate that training these architectures from scratch until convergence requires approximately 26.4 GPU hours.

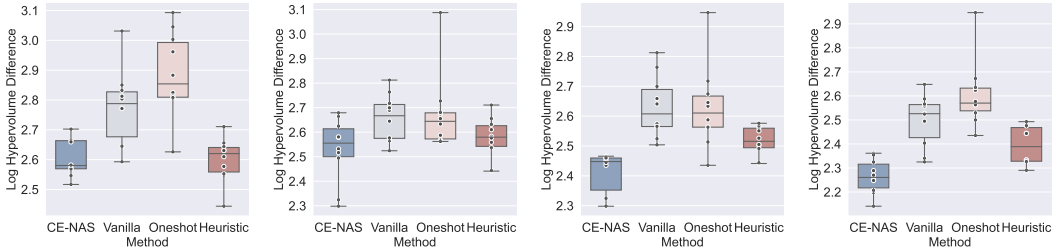

(a) CO_2 cost: 10000g (b) CO_2 cost: 20000g (c) CO_2 cost: 30000g (d) CO_2 cost: 50000g

Figure 4: Search efficiency under carbon emission constraints. These results are based on HW-NAS-Bench with carbon trace showing in fig. 2, and we ran each method ten times.

55]. The studies in [11, 56] employ a Feed-Forward Neural Network (FFNN) for their forecasts, while [55] utilizes a combination of FFNN, Convolutional Neural Network, and Long Short-Term Memory networks for multi-day carbon intensity predictions. We use the Mean Absolute Percentage Error (MAPE) to evaluate forecasting accuracy. Table 1 demonstrates a day-to-day comparison of all methods, with the most effective technique in bold. Our model demonstrates the best performance for both single-day and multi-day carbon intensity forecasting scenarios. More experimental details can be found in Appendix E.1.

4.2 NAS Benchmarks and Baselines

To date, there are three popular open-source NAS benchmarks, NasBench101 [90], HW-NAS-BENCH [28], and NasBench301 [93]. For our evaluation, we focus on the latter two, as the network architectures within these benchmarks cover the entirety of the search space. In contrast, the NasBench101 benchmark comprises only a limited subset of potential architectures. Evaluating using NasBench101 is challenging because we will not have access to important information, such as accuracy, during the search for the architecture not in the NasBench101 benchmark. We choose three types of baselines according to different GPU allocation strategies and NAS evaluation algorithms, including *vanilla LaMOO* [98], *one-shot LaMOO* [98] and a heuristic GPU allocation strategy [4], which is the SOTA result so far. We also define a carbon budget as the termination condition. Once the NAS exceeds this CO_2 budget, it will be stopped. More baseline details are in Appendix E.2.3.

4.2.1 Simulation using HW-NAS-Bench

Table 3: Search Results on ImageNet. The two optimization objectives we are searching for are TensorRT Latency with FP16 in NVIDIA V100 and accuracy.

Method	Top-1 Error(%)	TensorRT Latency FP16 V100 (ms)	Search&Training Cost (GPU Hours)†	CO2 (lbs)	NAS Method
NASNet-A [102]	26.0	2.86	48300	30679.13	vanilla
PNAS [45]	25.8	2.79	5700	4063.14	vanilla
MnasNet [71]	24.8	**0.53**	40300	26487.44	vanilla
AlphaX [79]	24.5	2.52	3900	2768.21	vanilla
AmoebaNet-C [66]	24.3	2.63	75900	44177.38	vanilla
AutoSlim [91]‡	25.8	1.64	480	321.89	one-shot
ProxylessNAS [14]‡	25.4	0.98	500	332.07	one-shot
SinglePathNAS [31]‡	25.3	1.13	686	455.99	one-shot
PC-DARTS [88]‡	24.2	1.50	411	278.15	one-shot
FBNet-C [83]‡	21.5	1.22	576	381.58	one-shot
OFA-Net [13]‡	20.0	1.16	1315	888.85	one-shot
CE-Net-G1‡	21.0	**0.56**	2706	909.86	hybrid
CE-Net-G2‡	**19.4**	0.78	2706	909.86	hybrid

† The total cost includes both the NAS search duration and the training time for the architectures identified.
‡ The architecture is searched on ImageNet directly, otherwise it is searched on CIFAR-10 by transfer setting.

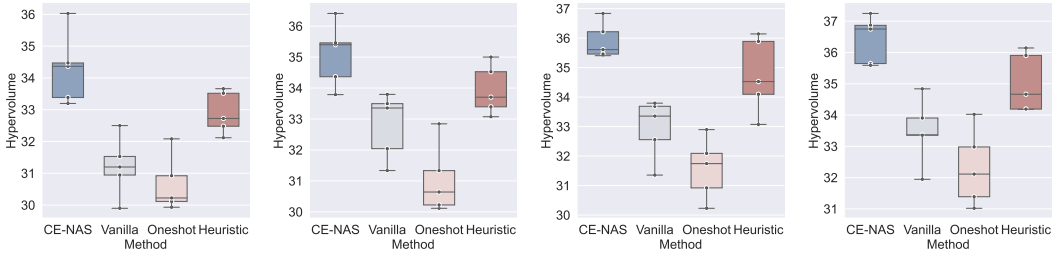

(a) CO_2 cost: 25000g (b) CO_2 cost: 50000g (c) CO_2 cost: 75000g (d) CO_2 cost: 100000g

Figure 5: Search efficiency under carbon emission constraints. These results are based on Nas-Bench301 with carbon trace showing in fig. 2, and we ran each method five times.

We evaluate our experimental results using two metrics: *relative carbon emission* and *log hypervolume difference*. Note that *log hypervolume difference* measures the quality of the search result and the smaller the better. Detailed definitions of these metrics can be found in Appendix E.2.4. As depicted in Figure 3(a), as the search time progresses, vanilla LaMOO demonstrates the highest performance in terms of $HV_{\text{log\_diff}}$. Vanilla LaMOO's superior performance can be attributed to its approach of *training all sampled architectures* to obtain their true accuracy, which effectively steers the search direction. However, when considering the relative carbon emission, vanilla LaMOO consumes 3.24X-7.22X carbon compared to other approaches. This is expected because vanilla LaMOO is an energy-intensive approach and is not designed to be aware of carbon emissions.

We show that `CE-NAS`'s search efficiency is only marginally lower than that of vanilla LaMOO while having the least relative carbon emission. Note that we are plotting the $HV_{\text{log\_diff}}$ in the Y-axis of Figure 3(a); the actual HV values achieved by `CE-NAS` and Vanilla LaMOO are about 4100 and 4117, differing only by 0.034%, even though the two lines look far apart. This result also suggests that only relying on energy-efficient approaches (e.g., one-shot LaMOO in this case) is insufficient to achieve good search performance. `CE-NAS` only takes 15 hours to get the comparable HV results with the final results of One-shot LaMOO.

Figure 4 presents a comparative analysis of `CE-NAS`'s performance against various baselines under differing carbon budgets. It is evident that `CE-NAS` surpasses all baselines in search efficiency under different CO_2 budget constraints[5]. Below a consumption level of 10,000g CO_2, Notably, the search outcomes associated with `CE-NAS`, as depicted in Figure 4(a), and those of vanilla/one-shot LaMOO, as shown in Figure 4(d), are comparable in terms of the median log hypervolume difference. This indicates that integrating `CE-NAS` with the NAS strategy can achieve a carbon cost saving of up to 5X compared to the conventional vanilla/one-shot NAS methodologies.

[5]We did not account for the carbon cost of training and inference for the RL models and the time-series transformer, as they consume negligible CO_2 compared to the NAS process.

https://doi.org/10.52202/079017-2628

4.2.2 Simulation using NasBench301

On NasBench301, we use two metrics: *relative carbon emission* and *hypervolume*(HV). Note that higher HV means better search results. Given the expansive nature of the NasBench301 search space, the maximal hypervolume remains undetermined. Consequently, rather than employing the hypervolume difference as a performance metric, we utilize the absolute hypervolume value to represent the efficacy of our search strategy. As depicted in Figure 3(b), our findings are consistent with those from HW-NasBench. One-shot LaMOO incurs the lowest carbon footprint but yields the least impressive performance in terms of hypervolume. Conversely, Vanilla LaMOO achieves the highest HV but at a carbon cost that exceeds CE-NAS by more than 3.76 times. CE-NAS markedly surpasses the SoTA heuristic GPU allocation strategy regarding HV, while maintaining a comparable carbon expenditure. At equivalent levels of carbon cost, as illustrated in Figure 5, CE-NAS demonstrates significantly superior search performance compared to other baselines. Figures 5(a) and 5(d) show that architectures identified through CE-NAS not only yield better results but also do so with a carbon cost that is four times lower than that of one-shot and vanilla NAS methods. Within the NasBench301 framework, CE-NAS also substantially outperforms the heuristic GPU allocation approach for NAS.

4.3 Open-Domain NAS Tasks

4.3.1 Searching on CIFAR-10 Image Classification Task

Our CE-NAS framework is compared with other popular NAS baselines, including vanilla and one-shot methods. Table 2 presents the SOTA results using DARTS and NASNet search spaces on CIFAR-10. The first group in the table comprises models discovered using vanilla NAS, and the second group includes those found with one-shot NAS. The CO_2 cost is calculated based on the duration of the search/training and the carbon intensity in the CISO region. For our CE-NAS, we select the optimal architectures from the Pareto frontier of the search results. Our CE-Net-P1 has only 1.68M parameters, significantly reducing parameter size compared to other baselines while maintaining a comparable top-1 accuracy (97.35%) with other SOTA models. Our CE-Net-P2 surpasses all baselines in top-1 accuracy (97.84%) while maintaining a similar parameter count of 3.26M. The performance discrepancy between the one-shot (second group) and vanilla NAS (first group) methods is attributed to the supernet's inaccurate accuracy prediction [31, 92]. Remarkably, our CE-NAS not only outperforms all vanilla-based NAS algorithms but also incurs a mere 38.53 lbs of CO_2 for the NAS search, comparable to the cost of one-shot-based NAS methods. More details related to the search space, training/search setup in More details in Appendix E.3.1.

4.3.2 Searching on ImageNet Image Classification Task

Table 3 demonstrates a comparison between our CE-NAS and other state-of-the-art (SOTA) baselines. We selected our searched models, designated as CE-Net-G1 and CE-Net-G2, from the Pareto frontier, based on the dual objectives of accuracy and TensorRT latency. Our searched architectures incur a slightly higher carbon cost (909.86 lbs) compared to one-shot-based SOTA baselines but significantly outperform these baselines in terms of top-1 accuracy and TensorRT latency. More details on search space, and training/search setup are demonstrated in Appendix E.3.2.

5 Conclusion

In this work, we described the design of a carbon-efficient NAS framework CE-NAS by leveraging the temporal variations in carbon intensity. To search for energy-efficient architectures, CE-NAS integrates a SOTA multi-objective optimizer, LaMOO [98], with the one/few-shot and vanilla NAS algorithms. These two NAS evaluation strategies have different energy requirements, which CE-NAS leverages an RL-based agent to schedule when to use each based on average carbon intensity. CE-NAS has demonstrated very promising results across various NAS tasks. For example, on CIFAR-10, CE-NAS successfully identified an architecture that achieves 97.35% top-1 accuracy with just 1.68M parameters and emitted only 38.53 lbs of CO_2. These compelling results suggest the efficacy and potential of CE-NAS as an effective framework in carbon-aware NAS. Additionally, on ImageNet, CE-NAS discovered state-of-the-art models achieving a top-1 accuracy of 80.6% with a TensorRT latency of 0.78 ms using FP16 on NVIDIA V100, and a top-1 accuracy of 79.0% with a latency of 0.56 ms on the same hardware. The carbon cost for this search was only 909.86 lbs.

6 Acknowledgement

This work was supported in part by NSF Grants #2105564 and #2236987, a VMware grant, the Worcester Polytechnic Institute's Computer Science Department, and the National Natural Science Foundation of China under No. 62072302. This work also used Expanse at San Diego Supercomputer Center through allocation CIS230364 from the Advanced Cyberinfrastructure Coordination Ecosystem: Services & Support (ACCESS) program, which is supported by National Science Foundation grants #2138259, #2138286, #2138307, #2137603, and #2138296.

References

[1] CO2Scrap, https://github.com/carbonfirst/CO2Scrap.

[2] Time series transformer, https://huggingface.co/docs/transformers/model_doc/time_series_transformer.

[3] Mohamed S Abdelfattah, Abhinav Mehrotra, Łukasz Dudziak, and Nicholas D Lane. Zero-cost proxies for lightweight nas. *arXiv preprint arXiv:2101.08134*, 2021.

[4] Anomynous Author(s). Anomynous title. In *Anomynous Venue*, 2023.

[5] Peter Auer, Nicolo Cesa-Bianchi, and Paul Fischer. Finite-time analysis of the multiarmed bandit problem. *Machine learning*, 47(2):235–256, 2002.

[6] Minkyung Baek, Frank DiMaio, Ivan Anishchenko, Justas Dauparas, Sergey Ovchinnikov, Gyu Rie Lee, Jue Wang, Qian Cong, Lisa N Kinch, R Dustin Schaeffer, et al. Accurate prediction of protein structures and interactions using a three-track neural network. *Science*, 373(6557):871–876, 2021.

[7] Yixin Bao, Yanghua Peng, and Chuan Wu. Deep learning-based job placement in distributed machine learning clusters. In *IEEE INFOCOM 2019 - IEEE Conference on Computer Communications*, pages 505–513, 2019.

[8] Yixin Bao, Yanghua Peng, and Chuan Wu. Deep learning-based job placement in distributed machine learning clusters with heterogeneous workloads. *IEEE/ACM Transactions on Networking*, 31(2):634–647, 2023.

[9] Noman Bashir, Tian Guo, Mohammad Hajiesmaili, David Irwin, Prashant Shenoy, Ramesh Sitaraman, Abel Souza, and Adam Wierman. Enabling sustainable clouds: The case for virtualizing the energy system. In *Proceedings of the ACM Symposium on Cloud Computing*, pages 350–358, 2021.

[10] Gabriel Bender, Pieter-Jan Kindermans, Barret Zoph, Vijay Vasudevan, and Quoc Le. Understanding and simplifying one-shot architecture search. In *Proceedings of the 35th International Conference on Machine Learning*, 10–15 Jul 2018.

[11] Neeraj Dhanraj Bokde, Bo Tranberg, and Gorm Bruun Andresen. Short-term co2 emissions forecasting based on decomposition approaches and its impact on electricity market scheduling. *Applied Energy*, 281:116061, 2021.

[12] Han Cai, Tianyao Chen, Weinan Zhang, Yong Yu, and Jun Wang. Efficient architecture search by network transformation. In *Proceedings of the AAAI conference on artificial intelligence*, volume 32, 2018.

[13] Han Cai, Chuang Gan, Tianzhe Wang, Zhekai Zhang, and Song Han. Once for all: Train one network and specialize it for efficient deployment. In *International Conference on Learning Representations*, 2020.

[14] Han Cai, Ligeng Zhu, and Song Han. ProxylessNAS: Direct neural architecture search on target task and hardware. In *International Conference on Learning Representations*, 2019.

[15] Jingxuan Chen, Xianbin Cao, Peng Yang, Meng Xiao, Siqiao Ren, Zhongliang Zhao, and Dapeng Oliver Wu. Deep reinforcement learning based resource allocation in multi-uav-aided mec networks. *IEEE Transactions on Communications*, 71(1):296–309, 2023.

 https://doi.org/10.52202/079017-2628

[16] Wuyang Chen, Xinyu Gong, and Zhangyang Wang. Neural architecture search on imagenet in four gpu hours: A theoretically inspired perspective. *arXiv preprint arXiv:2102.11535*, 2021.

[17] Wuyang Chen, Wei Huang, Xianzhi Du, Xiaodan Song, Zhangyang Wang, and Denny Zhou. Auto-scaling vision transformers without training. *arXiv preprint arXiv:2202.11921*, 2022.

[18] Xin Chen, Lingxi Xie, Jun Wu, and Qi Tian. Progressive DARTS: bridging the optimization gap for NAS in the wild. *CoRR*, abs/1912.10952, 2019.

[19] Zhaoyun Chen, Lei Luo, Wei Quan, Mei Wen, and Chunyuan Zhang. Poster abstract: Deep learning workloads scheduling with reinforcement learning on gpu clusters. In *IEEE INFOCOM 2019 - IEEE Conference on Computer Communications Workshops (INFOCOM WKSHPS)*, pages 1023–1024, 2019.

[20] Zheyi Chen, Jia Hu, Geyong Min, Chunbo Luo, and Tarek El-Ghazawi. Adaptive and efficient resource allocation in cloud datacenters using actor-critic deep reinforcement learning. *IEEE Transactions on Parallel and Distributed Systems*, 33(8):1911–1923, 2022.

[21] Xiangxiang Chu, Tianbao Zhou, Bo Zhang, and Jixiang Li. Fair DARTS: eliminating unfair advantages in differentiable architecture search. *CoRR*, abs/1911.12126, 2019.

[22] Jingjing Cui, Yuanwei Liu, and Arumugam Nallanathan. Multi-agent reinforcement learning-based resource allocation for uav networks. *IEEE Transactions on Wireless Communications*, 19(2):729–743, 2020.

[23] X. Dai, P. Zhang, B. Wu, H. Yin, F. Sun, Y. Wang, M. Dukhan, Y. Hu, Y. Wu, Y. Jia, P. Vajda, M. Uyttendaele, and N. K. Jha. Chamnet: Towards efficient network design through platform-aware model adaptation. In *2019 IEEE/CVF Conference on Computer Vision and Pattern Recognition (CVPR)*, pages 11390–11399, 2019.

[24] Samuel Daulton, Maximilian Balandat, and Eytan Bakshy. Differentiable expected hypervolume improvement for parallel multi-objective bayesian optimization. *arXiv preprint arXiv:2006.05078*, 2020.

[25] Samuel Daulton, Maximilian Balandat, and Eytan Bakshy. Parallel bayesian optimization of multiple noisy objectives with expected hypervolume improvement. *Advances in Neural Information Processing Systems*, 34:2187–2200, 2021.

[26] Tobias Domhan, Jost Tobias Springenberg, and Frank Hutter. Speeding up automatic hyperparameter optimization of deep neural networks by extrapolation of learning curves. In *Twenty-fourth international joint conference on artificial intelligence*, 2015.

[27] Jin-Dong Dong, An-Chieh Cheng, Da-Cheng Juan, Wei Wei, and Min Sun. Dpp-net: Device-aware progressive search for pareto-optimal neural architectures. In *Proceedings of the European Conference on Computer Vision (ECCV)*, pages 517–531, 2018.

[28] Xuanyi Dong and Yi Yang. Nas-bench-201: Extending the scope of reproducible neural architecture search. In *International Conference on Learning Representations (ICLR)*, 2020.

[29] Thomas Elsken, Jan Hendrik Metzen, and Frank Hutter. Efficient multi-objective neural architecture search via lamarckian evolution. *arXiv preprint arXiv:1804.09081*, 2018.

[30] Oliver Faust, Yuki Hagiwara, Tan Jen Hong, Oh Shu Lih, and U Rajendra Acharya. Deep learning for healthcare applications based on physiological signals: A review. *Computer methods and programs in biomedicine*, 161:1–13, 2018.

[31] Zichao Guo, Xiangyu Zhang, Haoyuan Mu, Wen Heng, Zechun Liu, Yichen Wei, and Jian Sun. Single path one-shot neural architecture search with uniform sampling. *CoRR*, abs/1904.00420, 2019.

[32] Xin He, Jiangchao Yao, Yuxin Wang, Zhenheng Tang, Ka Chu Cheung, Simon See, Bo Han, and Xiaowen Chu. Nas-lid: Efficient neural architecture search with local intrinsic dimension. *arXiv preprint arXiv:2211.12759*, 2022.

[33] James B Heaton, Nick G Polson, and Jan Hendrik Witte. Deep learning for finance: deep portfolios. *Applied Stochastic Models in Business and Industry*, 33(1):3–12, 2017.

[34] Shoukang Hu, Ruochen Wang, Lanqing HONG, Zhenguo Li, Cho-Jui Hsieh, and Jiashi Feng. Generalizing few-shot NAS with gradient matching. In *International Conference on Learning Representations*, 2022.

[35] Jian Huang, Junyi Chai, and Stella Cho. Deep learning in finance and banking: A literature review and classification. *Frontiers of Business Research in China*, 14(1):13, 2020.

[36] Aaron Klein, Stefan Falkner, Simon Bartels, Philipp Hennig, and Frank Hutter. Fast bayesian optimization of machine learning hyperparameters on large datasets. In *Artificial intelligence and statistics*, pages 528–536. PMLR, 2017.

[37] Namhoon Lee, Thalaiyasingam Ajanthan, and Philip HS Torr. Snip: Single-shot network pruning based on connection sensitivity. *arXiv preprint arXiv:1810.02340*, 2018.

[38] Sang Il Lee and Seong Joon Yoo. Multimodal deep learning for finance: integrating and forecasting international stock markets. *The Journal of Supercomputing*, 76:8294–8312, 2020.

[39] Baolin Li, Yankai Jiang, Vijay Gadepally, and Devesh Tiwari. Toward sustainable genai using generation directives for carbon-friendly large language model inference. *arXiv preprint arXiv:2403.12900*, 2024.

[40] Chaojian Li, Zhongzhi Yu, Yonggan Fu, Yongan Zhang, Yang Zhao, Haoran You, Qixuan Yu, Yue Wang, Cong Hao, and Yingyan Lin. {HW}-{nas}-bench: Hardware-aware neural architecture search benchmark. In *International Conference on Learning Representations*, 2021.

[41] Guihong Li, Duc Hoang, Kartikeya Bhardwaj, Ming Lin, Zhangyang Wang, and Radu Marculescu. Zero-shot neural architecture search: Challenges, solutions, and opportunities. *IEEE Transactions on Pattern Analysis and Machine Intelligence*, 2024.

[42] Weihe Li, Jiawei Huang, Wenjun Lyu, Baoshen Guo, Wanchun Jiang, and Jianxin Wang. Rav: Learning-based adaptive streaming to coordinate the audio and video bitrate selections. *IEEE Transactions on Multimedia*, 25:5662–5675, 2023.

[43] Heechul Lim, Min-Soo Kim, and Jinjun Xiong. {CNAS}: Channel-level neural architecture search, 2020.

[44] Ming Lin, Pichao Wang, Zhenhong Sun, Hesen Chen, Xiuyu Sun, Qi Qian, Hao Li, and Rong Jin. Zen-nas: A zero-shot nas for high-performance image recognition. In *Proceedings of the IEEE/CVF International Conference on Computer Vision*, pages 347–356, 2021.

[45] Chenxi Liu, Barret Zoph, Maxim Neumann, Jonathon Shlens, Wei Hua, Li-Jia Li, Li Fei-Fei, Alan L. Yuille, Jonathan Huang, and Kevin Murphy. Progressive neural architecture search. In *European Conference on Computer Vision(ECCV)*, 2018.

[46] Hanxiao Liu, Karen Simonyan, and Yiming Yang. DARTS: Differentiable architecture search. In *International Conference on Learning Representations(ICLR)*, 2019.

[47] Ning Liu, Zhe Li, Jielong Xu, Zhiyuan Xu, Sheng Lin, Qinru Qiu, Jian Tang, and Yanzhi Wang. A hierarchical framework of cloud resource allocation and power management using deep reinforcement learning. In *2017 IEEE 37th International Conference on Distributed Computing Systems (ICDCS)*, pages 372–382, 2017.

[48] Tong Liu, Shenggang Ni, Xiaoqiang Li, Yanmin Zhu, Linghe Kong, and Yuanyuan Yang. Deep reinforcement learning based approach for online service placement and computation resource allocation in edge computing. *IEEE Transactions on Mobile Computing*, 22(7):3870–3881, 2023.

[49] Yunzhuo Liu, Bo Jiang, Tian Guo, Ramesh K Sitaraman, Don Towsley, and Xinbing Wang. Grad: Learning for overhead-aware adaptive video streaming with scalable video coding. In *Proceedings of the 28th ACM International Conference on Multimedia*, 2020.

 https://doi.org/10.52202/079017-2628

[50] Vasco Lopes, Saeid Alirezazadeh, and Luís A Alexandre. Epe-nas: Efficient performance estimation without training for neural architecture search. In *International conference on artificial neural networks*, pages 552–563. Springer, 2021.

[51] Ilya Loshchilov and Frank Hutter. SGDR: stochastic gradient descent with restarts. *CoRR*, abs/1608.03983, 2016.

[52] Zhichao Lu, Kalyanmoy Deb, Erik Goodman, Wolfgang Banzhaf, and Vishnu Naresh Boddeti. Nsganetv2: Evolutionary multi-objective surrogate-assisted neural architecture search. In *Computer Vision – ECCV 2020: 16th European Conference, Glasgow, UK, August 23–28, 2020, Proceedings, Part I*, page 35–51, Berlin, Heidelberg, 2020. Springer-Verlag.

[53] Zhichao Lu, Ian Whalen, Vishnu Boddeti, Yashesh Dhebar, Kalyanmoy Deb, Erik Goodman, and Wolfgang Banzhaf. Nsga-net: neural architecture search using multi-objective genetic algorithm. In *Proceedings of the genetic and evolutionary computation conference*, pages 419–427, 2019.

[54] Renqian Luo, Fei Tian, Tao Qin, Enhong Chen, and Tie-Yan Liu. Neural architecture optimization. In *Advances in Neural Information Processing Systems 31*. 2018.

[55] Diptyaroop Maji, Prashant Shenoy, and Ramesh K. Sitaraman. Multi-day forecasting of electric grid carbon intensity using machine learning. *SIGENERGY Energy Inform. Rev.*, 3(2):19–33, jun 2023.

[56] Diptyaroop Maji, Ramesh K. Sitaraman, and Prashant Shenoy. Dacf: Day-ahead carbon intensity forecasting of power grids using machine learning. In *Proceedings of the Thirteenth ACM International Conference on Future Energy Systems*, e-Energy '22, page 188–192, New York, NY, USA, 2022. Association for Computing Machinery.

[57] Hongzi Mao, Ravi Netravali, and Mohammad Alizadeh. Neural adaptive video streaming with pensieve. In *Proceedings of the Conference of the ACM Special Interest Group on Data Communication*, SIGCOMM '17, 2017.

[58] Electricity Map. Electricity map.

[59] Joe Mellor, Jack Turner, Amos Storkey, and Elliot J Crowley. Neural architecture search without training. In *International conference on machine learning*, pages 7588–7598. PMLR, 2021.

[60] Riccardo Miotto, Fei Wang, Shuang Wang, Xiaoqian Jiang, and Joel T Dudley. Deep learning for healthcare: review, opportunities and challenges. *Briefings in bioinformatics*, 19(6):1236–1246, 2018.

[61] Volodymyr Mnih, Adria Puigdomenech Badia, Mehdi Mirza, Alex Graves, Timothy Lillicrap, Tim Harley, David Silver, and Koray Kavukcuoglu. Asynchronous methods for deep reinforcement learning. In *Proceedings of The 33rd International Conference on Machine Learning*, 2016.

[62] Yuqi Nie, Nam H Nguyen, Phanwadee Sinthong, and Jayant Kalagnanam. A time series is worth 64 words: Long-term forecasting with transformers. *arXiv preprint arXiv:2211.14730*, 2022.

[63] Ahmet Murat Ozbayoglu, Mehmet Ugur Gudelek, and Omer Berat Sezer. Deep learning for financial applications: A survey. *Applied soft computing*, 93:106384, 2020.

[64] Zhiping Peng, Delong Cui, Jinglong Zuo, Qirui Li, Bo Xu, and Weiwei Lin. Random task scheduling scheme based on reinforcement learning in cloud computing. *Cluster computing*, 18:1595–1607, 2015.

[65] Hieu Pham, Melody Y. Guan, Barret Zoph, Quoc V. Le, and Jeff Dean. Efficient neural architecture search via parameter sharing. In *International Conference on Machine Learning(ICML)*, 2018.

[66] Esteban Real, Alok Aggarwal, Yanping Huang, and Quoc V. Le. Regularized evolution for image classifier architecture search. In *Association for the Advancement of Artificial Intelligence(AAAI)*, 2019.

[67] Yoko Sasaki, Syusuke Matsuo, Asako Kanezaki, and Hiroshi Takemura. A3c based motion learning for an autonomous mobile robot in crowds. In *2019 IEEE International Conference on Systems, Man and Cybernetics (SMC)*, 2019.

[68] Emma Strubell, Ananya Ganesh, and Andrew McCallum. Energy and policy considerations for deep learning in nlp. *arXiv preprint arXiv:1906.02243*, 2019.

[69] Xiu Su, Shan You, Mingkai Zheng, Fei Wang, Chen Qian, Changshui Zhang, and Chang Xu. K-shot nas: Learnable weight-sharing for nas with k-shot supernets. In *International Conference on Machine Learning*, pages 9880–9890. PMLR, 2021.

[70] Zhenhong Sun, Ming Lin, Xiuyu Sun, Zhiyu Tan, Hao Li, and Rong Jin. Mae-det: Revisiting maximum entropy principle in zero-shot nas for efficient object detection. *arXiv preprint arXiv:2111.13336*, 2021.

[71] Mingxing Tan, Bo Chen, Ruoming Pang, Vijay Vasudevan, and Quoc V. Le. Mnasnet: Platform-aware neural architecture search for mobile. In *Conference on Computer Vision and Pattern Recognition(CVPR)*, 2019.

[72] Mingxing Tan and Quoc V. Le. Efficientnet: Rethinking model scaling for convolutional neural networks. *CoRR*, abs/1905.11946, 2019.

[73] Hidenori Tanaka, Daniel Kunin, Daniel L Yamins, and Surya Ganguli. Pruning neural networks without any data by iteratively conserving synaptic flow. *Advances in neural information processing systems*, 33:6377–6389, 2020.

[74] Lucas Theis, Iryna Korshunova, Alykhan Tejani, and Ferenc Huszár. Faster gaze prediction with dense networks and fisher pruning. *arXiv preprint arXiv:1801.05787*, 2018.

[75] Shreshth Tuli, Shashikant Ilager, Kotagiri Ramamohanarao, and Rajkumar Buyya. Dynamic scheduling for stochastic edge-cloud computing environments using a3c learning and residual recurrent neural networks. *IEEE Transactions on Mobile Computing*, 2022.

[76] Chaoqi Wang, Guodong Zhang, and Roger Grosse. Picking winning tickets before training by preserving gradient flow. *arXiv preprint arXiv:2002.07376*, 2020.

[77] Linnan Wang, Rodrigo Fonseca, and Yuandong Tian. Learning search space partition for black-box optimization using monte carlo tree search. *Advances in Neural Information Processing Systems*, 33:19511–19522, 2020.

[78] Linnan Wang, Saining Xie, Teng Li, Rodrigo Fonseca, and Yuandong Tian. Sample-efficient neural architecture search by learning action space. *CoRR*, abs/1906.06832, 2019.

[79] Linnan Wang, Yiyang Zhao, Yuu Jinnai, Yuandong Tian, and Rodrigo Fonseca. Alphax: exploring neural architectures with deep neural networks and monte carlo tree search. *CoRR*, abs/1903.11059, 2019.

[80] Xiaoxing Wang, Chao Xue, Junchi Yan, Xiaokang Yang, Yonggang Hu, and Kewei Sun. Mergenas: Merge operations into one for differentiable architecture search. In Christian Bessiere, editor, *Proceedings of the Twenty-Ninth International Joint Conference on Artificial Intelligence, IJCAI 2020*, pages 3065–3072. ijcai.org, 2020.

[81] Joseph L Watson, David Juergens, Nathaniel R Bennett, Brian L Trippe, Jason Yim, Helen E Eisenach, Woody Ahern, Andrew J Borst, Robert J Ragotte, Lukas F Milles, et al. De novo design of protein structure and function with rfdiffusion. *Nature*, 620(7976):1089–1100, 2023.

[82] Xuekai Wei, Mingliang Zhou, Sam Kwong, Hui Yuan, Shiqi Wang, Guopu Zhu, and Jingchao Cao. Reinforcement learning-based qoe-oriented dynamic adaptive streaming framework. *Information Sciences*, 569:786–803, 2021.

 https://doi.org/10.52202/079017-2628

[83] Bichen Wu, Xiaoliang Dai, Peizhao Zhang, Yanghan Wang, Fei Sun, Yiming Wu, Yuandong Tian, Peter Vajda, Yangqing Jia, and Kurt Keutzer. Fbnet: Hardware-aware efficient convnet design via differentiable neural architecture search. *The IEEE Conference on Computer Vision and Pattern Recognition (CVPR)*, 2019.

[84] Haixu Wu, Jiehui Xu, Jianmin Wang, and Mingsheng Long. Autoformer: Decomposition transformers with auto-correlation for long-term series forecasting. *Advances in Neural Information Processing Systems*, 34:22419–22430, 2021.

[85] Meng-Ting Wu and Chun-Wei Tsai. Training-free neural architecture search: a review. *ICT Express*, 2023.

[86] Dongkuan Xu, Subhabrata Mukherjee, Xiaodong Liu, Debadeepta Dey, Wenhui Wang, Xiang Zhang, Ahmed Hassan Awadallah, and Jianfeng Gao. Few-shot task-agnostic neural architecture search for distilling large language models. In Alice H. Oh, Alekh Agarwal, Danielle Belgrave, and Kyunghyun Cho, editors, *Advances in Neural Information Processing Systems*, 2022.

[87] Jingjing Xu, Liang Zhao, Junyang Lin, Rundong Gao, Xu Sun, and Hongxia Yang. Knas: green neural architecture search. In *International Conference on Machine Learning*, pages 11613–11625. PMLR, 2021.

[88] Yuhui Xu, Lingxi Xie, Xiaopeng Zhang, Xin Chen, Guo-Jun Qi, Qi Tian, and Hongkai Xiong. {PC}-{darts}: Partial channel connections for memory-efficient architecture search. In *International Conference on Learning Representations*, 2020.

[89] Hao Ye, Geoffrey Ye Li, and Biing-Hwang Fred Juang. Deep reinforcement learning based resource allocation for v2v communications. *IEEE Transactions on Vehicular Technology*, 68(4):3163–3173, 2019.

[90] Chris Ying, Aaron Klein, Eric Christiansen, Esteban Real, Kevin Murphy, and Frank Hutter. NAS-bench-101: Towards reproducible neural architecture search. In *Proceedings of the 36th International Conference on Machine Learning*, 2019.

[91] Jiahui Yu and Thomas S. Huang. Network slimming by slimmable networks: Towards one-shot architecture search for channel numbers. *CoRR*, abs/1903.11728, 2019.

[92] Kaicheng Yu, Christian Sciuto, Martin Jaggi, Claudiu Musat, and Mathieu Salzmann. Evaluating the search phase of neural architecture search. *arXiv preprint arXiv:1902.08142*, 2019.

[93] Arber Zela, Julien Niklas Siems, Lucas Zimmer, Jovita Lukasik, Margret Keuper, and Frank Hutter. Surrogate NAS benchmarks: Going beyond the limited search spaces of tabular NAS benchmarks. In *International Conference on Learning Representations*, 2022.

[94] Yu Zhang, Jianguo Yao, and Haibing Guan. Intelligent cloud resource management with deep reinforcement learning. *IEEE Cloud Computing*, 4(6):60–69, 2017.

[95] Zhihao Zhang and Zhihao Jia. Gradsign: Model performance inference with theoretical insights. *arXiv preprint arXiv:2110.08616*, 2021.

[96] Xiaoyang Zhao and Chuan Wu. Large-scale machine learning cluster scheduling via multi-agent graph reinforcement learning. *IEEE Transactions on Network and Service Management*, 19(4):4962–4974, 2022.

[97] Yiyang Zhao, Linnan Wang, Yuandong Tian, Rodrigo Fonseca, and Tian Guo. Few-shot neural architecture search. In *Proceedings of the 38th International Conference on Machine Learning*, volume 139 of *Proceedings of Machine Learning Research*, pages 12707–12718. PMLR, 18–24 Jul 2021.

[98] Yiyang Zhao, Linnan Wang, Kevin Yang, Tianjun Zhang, Tian Guo, and Yuandong Tian. Multi-objective optimization by learning space partition. In *International Conference on Learning Representations*, 2022.

[99] Haoyi Zhou, Shanghang Zhang, Jieqi Peng, Shuai Zhang, Jianxin Li, Hui Xiong, and Wancai Zhang. Informer: Beyond efficient transformer for long sequence time-series forecasting. In *Proceedings of the AAAI conference on artificial intelligence*, volume 35, pages 11106–11115, 2021.

[100] Hongpeng Zhou, Minghao Yang, Jun Wang, and Wei Pan. BayesNAS: A Bayesian approach for neural architecture search. In Kamalika Chaudhuri and Ruslan Salakhutdinov, editors, *Proceedings of the 36th International Conference on Machine Learning*, volume 97 of *Proceedings of Machine Learning Research*, pages 7603–7613. PMLR, 09–15 Jun 2019.

[101] Huan Zhou, Zhenning Wang, Hantong Zheng, Shibo He, and Mianxiong Dong. Cost minimization-oriented computation offloading and service caching in mobile cloud-edge computing: An a3c-based approach. *IEEE Transactions on Network Science and Engineering*, 2023.

[102] Barret Zoph, Vijay Vasudevan, Jonathon Shlens, and Quoc Le. Learning transferable architectures for scalable image recognition. In *Conference on Computer Vision and Pattern Recognition (CVPR)*, 2018.

 https://doi.org/10.52202/079017-2628

A Background Knowledge

A.1 Multi-objective NAS

Multi-objective NAS has gained popularity in the NAS community, as deep neural networks need to address not only traditional metrics like accuracy but also practical efficiency metrics. There are two main approaches within Multi-objective NAS. The first category [83, 71, 13, 23, 27] leverages linear scalarization of various metrics (e.g., $\frac{accuracy}{\#FLOPs}$) into a single metric, followed by the application of standard single-objective NAS algorithms for architecture search. The second category [98, 53, 52] approaches MONAS as a multi-objective black-box optimization problem. According to existing results [98, 52], this latter approach generally outperforms the former in terms of effectiveness and performance. For multi-objective optimization, mathematically, we optimize M objectives $\boldsymbol{f}(\boldsymbol{x}) = [f_1(\boldsymbol{x}), f_2(\boldsymbol{x}), \ldots, f_M(\boldsymbol{x})] \in \mathrm{r}^M$:

$$\begin{aligned} \min \quad & f_1(\boldsymbol{x}), f_2(\boldsymbol{x}), ..., f_M(\boldsymbol{x}) \\ \text{s.t.} \quad & \boldsymbol{x} \in \Omega, \end{aligned} \tag{2}$$

where $\boldsymbol{x}$ represents the neural architecture from the search space, $f_i(\boldsymbol{x})$ denotes the function of objective i. Modern MOO methods aim to find the problem's entire *Pareto frontier*, the set of solutions that are not *dominated* by any other feasible solutions. Here we define *dominance* $\boldsymbol{y} \prec_{\boldsymbol{f}} \boldsymbol{x}$ as $f_i(\boldsymbol{x}) \leq f_i(\boldsymbol{y})$ for all metrics f_i, and there exists at least one i s.t. $f_i(\boldsymbol{x}) < f_i(\boldsymbol{y})$, $1 \leq i \leq M$. If the condition holds, a solution $\boldsymbol{x}$ is always better than solution $\boldsymbol{y}$.

Table 4: Comparison of energy-efficient NAS evaluation methods. *Eval. cost* refers to the cost of obtaining the evaluation results. *Init. cost* describes additional dataset preparation and the time required for training the model (e.g., supernet or predictor). *Accuracy* measures the rank correlation between the evaluation method and the actual rank. Predictor-based methods require *Extra data* as a training set to construct the prediction model.

Method	Eval. cost	Init. cost	Accuracy	Extra data
Zero-shot proxy [41, 85, 50, 59, 44, 70, 16, 17]	Low	Low	Low	No
One-shot [46, 65, 97, 88, 13]	Low	Low	Intermediate	No
Predictor [45, 26, 79]	Low	High†	High†	Yes
Low-fidelity [102, 66, 46, 79, 36]	High	None	High‡	No
Gradient Proxy [87]	Low	Low	Intermediate	No

† It depends on the size of extra data.
‡ It depends on the extent of the fidelity.

A.2 One (few)-shot NAS

One (few)-shot NAS utilizes a weight-sharing technique, avoiding the need to retrain sampled networks from scratch. Specifically, one-shot NAS initially trains an over-parameterized *supernet*, including all possible operations and connections within the entire search space, and employs this supernet as a performance estimator to predict an architecture's efficacy [10, 92, 97, 65]. The performance of any architecture within the search space can be approximated by leveraging the well-trained supernet. Few-shot NAS [97, 34, 86, 32, 69] further improves the accuracy of architecture evaluations conducted by supernets. It achieves this by using multiple sub-supernets, thereby reducing the co-adaptation impact among operations [10]. In this work, we employ this few-shot supernet as an efficient proxy for architecture evaluation, with more details provided in Section 3.3.

A.3 Zero shot proxy NAS

Zero-shot NAS leverages training-free score functions/proxies to efficiently evaluate the performance of neural architectures [41, 85]. Compared to vanilla NAS and one/few-shot NAS, zero-shot NAS is cost-effective due to its training-free nature at the search stage. However, the main disadvantage of zero-shot NAS is its evaluation performance, which can be very inaccurate compared to one/few-shot NAS and vanilla NAS [41].

A.4 Reinforcement learning (RL)

RL has been widely used for designing system strategies for tasks such as scheduling and resource allocation. For instance, RL has been deployed to develop resource allocation strategies in wireless networks [22, 89, 15, 48] and cloud platforms [19, 47, 94, 20], as well as for making bitrate decisions in adaptive video streaming systems [57, 49, 42, 82], and also generating task scheduling strategies in data centers [64, 7, 96, 8]. The key advantage of RL-based methods is their capability to learn strategies and easily adapt to system changes automatically. An RL agent begins by taking the system state as input and proceeds to generate an action, i.e. a scheduling or allocation decision, based on its learned strategies, which is typically randomized at the start. Upon execution of the action, the system provides feedback in the form of a reward, enabling the RL agent to refine its strategies. The key to applying RL lies in the design of effective state inputs, actions, and rewards according to the specific task. Our `CE-NAS` focuses on tailoring these elements for carbon-efficient NAS tasks, with the guiding principle of simplifying the state and action spaces to expedite efficient and rapid training.

B Learning Search Space Partition

We utilize LaMOO [98] to partition the search space, Ω, into several sub-search spaces. This partitioning will be based on the architectures' accuracy $E(a)$ and their evaluation metrics $T(a)$ as observed in the sample set, $\mathcal{P}$. Specifically, LaMOO recursively divides the search space into promising and non-promising regions. Each partitioned region can then be mapped to a node in a search tree. Using Monte-Carlo Tree Search (MCTS), LaMOO selects the most promising sub-space (i.e., tree node) for further exploration based on their UCB values [5]. This optimal sub-space selected by MCTS is denoted as Ω_{best}.

C Details of Reinforcement Learning Based GPU Allocation Strategy

State Input. We design the RL state input at time step t as $s_t = (b_t, n_t, h_t, \mathbf{c_t})$, where b_t is the remaining carbon budget of the current searching task, n_t is the number of already searched architectures, h_t is the hypervolume of these architectures, and $\mathbf{c_t}$ is the future carbon traces in the upcoming hour (e.g., predicted by our time series transformer from §3.5.2). The general idea is that being aware of b_t helps the RL algorithm plan the overall amount of carbon emission to spend for architecture evaluation, while n_t, h_t and $\mathbf{c_t}$ help it decide the best timing to execute the evaluation that generates the highest hypervolume improvements per carbon cost.

Network architecture. Our network consists of an input layer, 2 hidden layers, and an output layer. All of the layers are fully connected layers, with hidden sizes of 100, 150, 200 and 100 respectively, which are determined by performing a simple grid search. The final output of the network specifies the probability of distribution of actions.

Action. We design the output of the RL agent as K discrete actions, i.e. the output is a vector $\mathbf{o_t} =< o_t^1, o_t^2, ..., o_t^K >$, where o_t^k denotes the probability of allocating a ratio of $\frac{(k-1)}{K}$ GPUs for architecture evaluation. We use K = 8 for our evaluation. We also implement a version of the agent with continuous action space, i.e., the network outputs the mean μ and standard σ of a Gaussian distribution to indicate the probability distribution of the GPU allocation ratio. Our evaluation in §F.4 shows that the two versions achieve comparable performance.

Rewards. As the overall goal is to maximize the cumulative reward that represents the final accuracy obtained by the search task, we design the reward in each time step as the improvement of the best accuracy of the already searched architectures: $r_t = (co_t, hi_t, nn_t)$, where co_t denotes the carbon cost in this iteration, hi_t represents the hypervolume increase in this iteration, and nn_t means the number of new samples in this step.

Policy gradient. We adopt the popular *actor-critic* algorithm to calculate the policy gradient and update the network. *Actor-critic* has been proved to achieve good performance while enabling fast training in tasks of similar scales [57, 49, 75, 67, 101]. Note that our design is not coupled with any specific DRL algorithm. Thus, replacing *actor-critic* with other algorithms is easy if needed. The key

 https://doi.org/10.52202/079017-2628

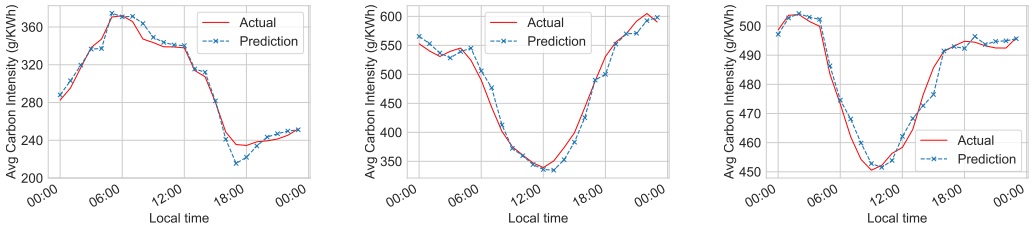

(a) Region: CISO (b) Region: DE (c) Region: PJM

Figure 6: Transformer-based carbon intensity predictor. Our predictor makes forecasts that perfectly match actual values over three different regions.

gradient equation of *actor-critic* is as follows:

$$\nabla E_{\pi_\theta}\left[\sum_{t=0}^{\infty}\gamma^t r_t\right] = E_{\pi_\theta}[\nabla_\theta \log \pi_\theta(s,a) A^{\pi_\theta}(s,a)] \tag{3}$$

where $\sum_{t=0}^{\infty}\gamma^t r_t$ is the cumulative rewards and γ is a discount factor. *Actor-critic* algorithm includes two networks referred to as *actor* and *critic* respectively. In our design, they use the same network structure. The *actor* is responsible for outputting $\pi_\theta(s,a)$, which is the output probability for action a with input state s. The policy parameter θ is the network parameter of the *actor*. $A^{\pi_\theta}(s,a)$ is the *advantage function* that indicates the performance difference between the current policy and the average performance of policies learned by *actor*. $A^{\pi_\theta}(s,a)$ is obtained with the *temporal difference* method based on the output of the *critic*. The calculation is as follows,

$$A(s_t,a_t) = r_t + \gamma V^{\pi_\theta}(s_{t+1};\theta_v) - V^{\pi_\theta}(s_t;\theta_v) \tag{4}$$

where $A(s_t,a_t)$ is an unbiased estimation of $A^{\pi_\theta}(s,a)$, θ_v is the parameter of the critic. $V^{\pi_\theta}(s_t;\theta_v)$ is the output of *critic* that estimates the cumulative reward follow actor policy π_θ starting from state s_t.

D Architecture Design of Time series Transformer

Building upon the foundational design of the time series Transformer, we employ LaMOO [98] as our NAS strategy to identify the optimal architectural parameters for our carbon dataset [58]. Our goal is to devise an architecture that not only achieves high forecasting accuracy but also maintains efficient training and latency times. Given that we are working with a standard encoder-decoder Transformer, our search space is straightforward. We focus on searching for: i) the number of encoder layers, ii) the number of decoder layers, iii) the embedding size, and iv) the maximum context length of the time series that the model is capable of considering. Following our NAS search process, we configured a model with 64 encoder layers, 96 decoder layers, with an embedding size of 48. Additionally, we set the context length to 8760.

E Experimental Details in Sec. 4

E.1 Time-series Transformer for Carbon Forcasting

We align our training and testing data with the approach used in [55] by utilizing ElectricityMap [58], a third-party carbon information service. We select three regions (namely, CISO[6], DE[7], and PJM[8]) from ElectricityMap [58] to represent distinct carbon trace scenarios for our experiments. The dataset spans from January 1, 2020, to December 31, 2021, with an hourly resolution. We employ a train(validation)-test split of 75%–25%. We trained a single transformer model using data from three

[6]CISO: California Independent System Operator
[7]DE: Germany
[8]PJM: Pennsylvania-Jersey-Maryland Interconnection

different regions simultaneously. Additionally, we conducted separate training sessions for the model using distinct traces from each location. The experimental results from both approaches were similar.

In our training configuration, the context length is set to 8760, as determined by our NAS search. We utilize the AdamW optimizer, setting the weight decay to 1×10^{-2} and selecting beta1 as 0.9 for the exponential decay rate of the first moment estimates, and beta2 as 0.95 for the second moment estimates. The model is trained over 150 epochs with an initial learning rate of 6×10^{-4}. The batch size is configured at 512 on a single NVIDIA A100 GPU.

For testing, to predict carbon intensity for the forthcoming 24 hours, we use all historical data up to the last complete 24-hour block. This block is then replaced with predictions from our model to forecast the carbon intensity for the 25th hour. Subsequent forecasts are generated by updating the most recent hour with its actual value and using the model's prediction for the next hour. We measure forecasting performance using the Mean Absolute Percentage Error (MAPE). For multi-day forecasts, we similarly update and replace values for the 24-, 48-, and 72-hour marks.

Figure 6 presents the hourly time series, averaged over a week, demonstrating both actual and predicted carbon intensities for the electricity grids in these areas. The comparison suggests that our model accurately forecasts the actual carbon trace in each region, aligning closely with the observed data.

E.2 Experimental Details on NAS Dataset

E.2.1 Overview of HW-NAS-Bench

HW-NAS-Bench [40] enhances the original NasBench201 dataset by including additional metrics such as inference latency, parameter size, and number of FLOPs, thereby expanding the evaluative dimensions available for NAS research. NasBench201 itself is a comprehensive open-source benchmark designed for the systematic assessment of NAS algorithms [28]. Within NasBench201, architectures are constructed by stacking cells in sequence. Specifically, each cell is composed of 4 nodes interconnected by 6 edges. Nodes represent feature maps, while edges correspond to various operations that transform one node's output into the next node's input. Operations connecting nodes include zeroization, skip-connection, 1x1 convolution, 3x3 convolution, and 3x3 average pooling. To uniquely identify each architecture, we employ a numeric encoding scheme where the five operations are represented by integers 0 through 4. Consequently, a 6-element vector represents the specific architecture.

E.2.2 Overview of NasBench301

NasBench301 [93] serves as a surrogate benchmark for the NASNet [102] search space, which has over 10^{21} possible architectures. NasBench301 employs a surrogate model trained on approximately 60,000 sampled architectures to predict performance across the entire DARTS [46] search space for the CIFAR-10 image classification task. This surrogate model within NasBench301 has been shown to provide accurate regression outcomes, facilitating reliable evaluations within this vast search space. NasBench301 offers predicted accuracies from the surrogate model, while other fundamental metrics such as the number of parameters (#Params), floating-point operations per second (#FLOPs), and inference time are readily ascertainable during the evaluation phase. In this multi-objective optimization context, our goal is to simultaneously maximize inference accuracy and minimize #Params within the NasBench301 search space.

The NASNet search space includes operations such as 3x3 max pool, 3x3 convolutions, 5x5 depth-separable convolutions, and skip connections. The objective here is to identify optimal architectures for both reduction and normal cells, each comprising 4 nodes, culminating in a search space of approximately 3.5×10^{21} architectures [93, 78]. For the CIFAR-10 task, we adopt the same encoding strategy used in the NASNet search space, representing architectures as 16-digit vectors. The first four digits denote the operations in a normal cell, digits 5-8 correspond to the concatenation patterns in the normal cell, digits 9-12 represent operations in a reduction cell, and the final four digits encode the concatenation patterns in the reduction cell.

 https://doi.org/10.52202/079017-2628

E.2.3 Baselines

We chose three types of baselines according to different GPU allocation strategies and NAS evaluation algorithms. During the search process, all search methods employ the state-of-the-art multi-objective optimizer, LaMOO [98]. Specifically, *one-shot LaMOO* is a method that utilizes one-shot evaluations throughout the search process. The *vanilla LaMOO* relies on actual training for architecture evaluation throughout the search.

We also provide a heuristic strategy that automatically allocates GPU resources between the sampling and evaluation processes given the carbon emissions C_t at time t as our baseline. This allocation is based on the energy characteristics of the processes: architecture sampling is often energy-efficient because it does not involve actual training of architectures, while architecture evaluation is often energy-consuming because it does. We assume that the maximum and minimum carbon intensities C_{max} and C_{min} for a future time window are known. G_t denotes the total number of available GPUs. λ_e and λ_s represent the ratio of GPU numbers allocated to the evaluation and sampling processes at a given moment, and $\lambda_e + \lambda_s = 1$. We calculate λ_s as $\frac{C_{cur}-C_{min}}{C_{max}-C_{min}}$, where C_{cur} is the current carbon intensity. The GPU allocations for the sampling and evaluation processes are, therefore, $G_t * \lambda_s$ and $G_t * \lambda_e$. This simple heuristic allocation allows the NAS system to prioritize more energy-efficient sampling tasks during periods of higher carbon intensity, whereas, during low-carbon periods, the system will allocate more resources for energy-intensive evaluation tasks.

E.2.4 Metrics in HW-NAS-Bench

We use two main metrics to evaluate the carbon and search efficiency of `CE-NAS`. First, we use *relative carbon emission* to quantify the amount of CO_2 each NAS method is responsible for. The relative carbon emission is calculated by summing the average carbon intensity (in gCO2/KwH) over the search process. We assume that all NAS methods use the same type of GPU whose power consumption remains the same throughout the search process. Second, we use the metric *hypervolume* (HV) to measure the "goodness" of searched samples. HV is a commonly used multi-objective optimization quality indicator [24, 25, 98] that considers all dimensions of the search objective. Given a reference point $R \in \mathrm{r}^M$, the HV of a finite approximate Pareto set $\mathcal{P}$ is the M-dimensional Lebesgue measure λ_M of the space dominated by $\mathcal{P}$ and bounded from below by R. That is, $HV(\mathcal{P}, R) = \lambda_M(\cup_{i=1}^{|\mathcal{P}|}[R, y_i])$, where $[R, y_i]$ denotes the hyper-rectangle bounded by the reference point R and y_i. A higher hypervolume denotes better multi-objective results. In this experiment, we calculate the hypervolume (HV) using the accuracy and inference energy of the searched architectures. For this dataset, we use the *log hypervolume* difference, the same as in [24, 25, 98], as our evaluation criterion for HW-NASBench, since the hypervolume difference may be minimal over the search process. Therefore, using log hypervolume allows us to visualize the sample efficiency of different search methods. We define $HV_{\text{log\_diff}} := \log(HV_{\max} - HV_{\text{cur}})$ where $HV_{\max}$ represents the maximum hypervolume calculated from all points in the search space, and HV_{cur} denotes the hypervolume of the current samples, which are obtained by the algorithm within a specified budget. The $HV_{\max}$ in this problem is 4150.7236.

For our simulation, we use the training and evaluation time costs for the architectures derived from NasBench201 [28], and inference energy costs measured on the NVIDIA Edge GPU Jetson TX2 from HW-NASBench [40]. We ran the simulation 10 times with each method.

E.2.5 Metrics in NasBench301

Given the expansive nature of the NasBench301 search space, the maximal hypervolume remains undetermined. Consequently, rather than employing the hypervolume difference as a performance metric, we utilize the absolute hypervolume value to represent the efficacy of our search strategy.

E.3 Experimental Details on Open-Domain NAS Tasks

E.3.1 Details on Cifar10 Image Classification Task

Search space overview. Our search space is consistent with the NASNet search space [102]. It comprises eight searchable operations: 3x3 max pooling, 3x3 average pooling, 3x3, 5x5, and 7x7 depthwise convolutions, 3x3 and 5x5 dilated convolutions, and a skip connection. The architecture consists of normal cells, which retain the size of the feature map, and reduction cells, which double

the channel size and halve the feature map resolution. Each cell integrates four nodes connected by eight different operations. The search space encompasses a total of 10^{21} architectures. We employ the same encoding strategy as prior studies [78].

Search setup We implement low-fidelity estimation methods [102, 66, 79] to expedite the energy-consuming evaluation part in the neural architecture search process. This approach effectively accelerates the evaluation process using cost-effective approximations while largely preserving the true relative ranking of the searched architectures. Initially, we utilize early stopping for training sampled architectures for 200 epochs, in contrast to 600 epochs required for the final training phase. To further hasten training, we reduce the initial channel size from 36 to 18 and increase the batch size to 320. Additionally, the number of layers is scaled down from 24 to 16 during the search phase. To speed up the evaluation process, we use the NVIDIA Automatic Mixed Precision (AMP) library with FP16 for training during the search.

We utilize a pre-trained reinforcement learning model based on data from NasBench201 and continually tune this model during the NAS process according to task-specific data. The carbon budget for the search is set at 100 lbs.

Training setup The final selected architectures are trained for 600 epochs, using a batch size of 128 and a momentum SGD optimizer with an initial learning rate of 0.025. This rate is adjusted following a cosine learning rate schedule throughout the training. Weight decay is applied for regularization.

E.3.2 Details on ImageNet

Search space overview. Our ImageNet search space is modeled after EfficientNet [72]. Specifically, it includes 5-8 stages for each architecture, with the number of stages being determined by NAS. From stages 3 to 8, the type of stage, either Fused-Inverse-Residual-Block (Fused-IRB) or Inverse-Residual-Block (IRB), is searchable. Within each stage, searchable parameters include activation type (e.g., ReLU, Swish), kernel size (e.g., 1, 3, 5, 7), number of layers ([1, 10]), expansion rate ([2, 7]), and number of channels (varies based on the stage). Additionally, our search space considers input image resolutions (e.g., 224, 288, 320, 384, 456, 528). The total search space size is approximately 10^{31}. Our NAS search focuses on two objectives: top-1 accuracy and TensorRT latency with FP16 on an NVIDIA V100. For TensorRT latency, we fixed the workspace at 10GB for all runs and benchmarked latency using a batch size of 1 with explicit shape configuration, reporting the average latency from 1000 runs.

Search setup As with CIFAR-10, we implement low-fidelity estimation methods [102, 66, 79] to accelerate the energy-consuming evaluation part in the neural architecture search process. Sampled architectures are trained for 150 epochs using early stopping, as opposed to the 450 epochs required in the final training phase. During the evaluation in the search process, we also reduce the channel size by a factor of 4. To further speed up the evaluation process, we leverage AMP with FP16 for training searched architectures.

Consistent with our CIFAR-10 approach, we employ a pre-trained reinforcement learning model based on data from NasBench201 and continually fine-tune this model during the NAS process using ImageNet task data. The carbon budget for the search is set at 1000 lbs.

Training setup For each architecture in the Pareto frontier, we train it on 8 Tesla V100 GPUs with a resolution of 320x320 in our two-objective accuracy and TensorRT latency. We utilize a standard SGD optimizer with Nesterov momentum of 0.9 and set the weight decay at 3×10^{-5}. Each architecture undergoes training for a total of 450 epochs, with the initial 10 epochs serving as the warm-up period. During these warm-up epochs, we apply a constant learning rate of 0.01. The remaining epochs are trained with an initial learning rate of 0.1, using a cosine learning rate decay schedule [51], and a batch size of 1024 (i.e., 128 images per GPU). The model parameters undergo decay at a factor of 0.9997 to further enhance our models' training performance.

F Ablation Studies

F.1 Effectiveness of LaMOO for NAS

We conducted ten runs of LaMOO (i.e., search space split) with a random search on the HW-NASBench dataset [40]. In addition, we performed random sampling for both the LaMOO-selected

 https://doi.org/10.52202/079017-2628

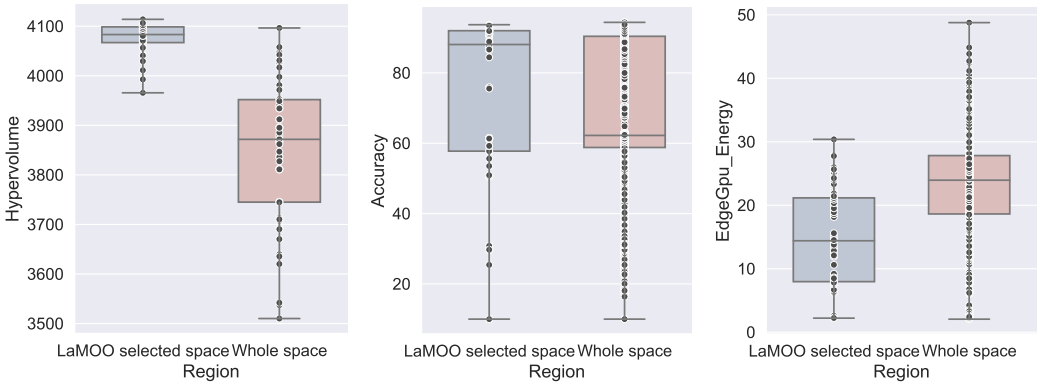

(a) Hypervolume (b) Accuracy (c) Inference energy

Figure 7: Comparisons of architecture qualities between LaMOO-selected region and the entire search space of HW-Nasbench. We ran LaMOO 10 times. For each run, we randomly sampled 50 architectures from the LaMOO-selected space and the whole search space.

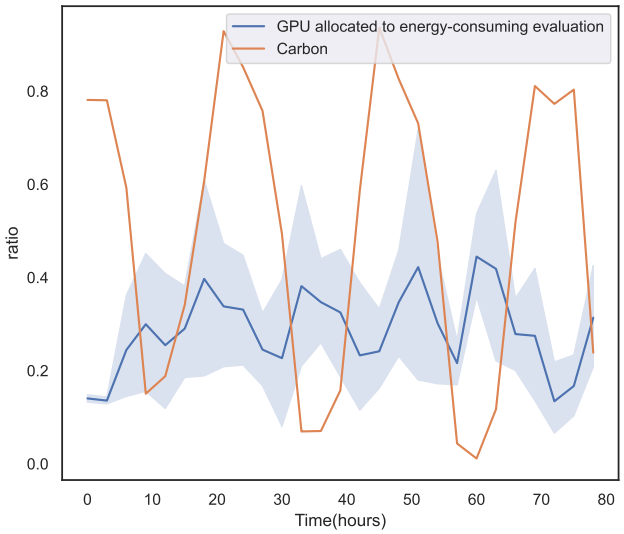

Figure 8: An overview of CE-NAS. This carbon trace and GPU ratio.

region and the entire search space, conducting 50 trials for each. The distribution of accuracy and edge GPU energy consumption of the architectures in both the LaMOO selected region and the entire search space can be seen in Figure 7.

Specifically, our results show that the architectures in the region selected by LaMOO have higher average accuracy and lower average edge GPU energy consumption compared to those in the entire search space. On average, the accuracy of the architectures in the LaMOO selected region is 72.12, while the accuracy in the entire search space is 68.28. The average edge GPU energy for the LaMOO selected region is 16.59 mJ, as opposed to 22.84 mJ for the entire space.

Furthermore, as illustrated in Figure 7(a), we observe that searching within the LaMOO-selected region yielded a tighter distribution, and the median hypervolume demonstrated an improvement compared to searching across the entire search space. These results suggest the efficacy of using LaMOO to partition the search space for NAS.

https://doi.org/10.52202/079017-2628

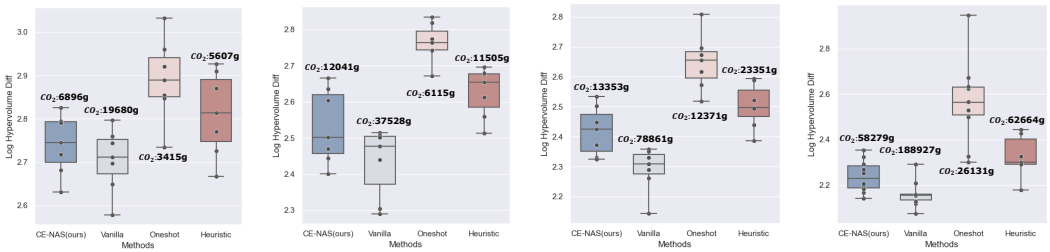

(a) Search budget:10 hrs (b) Search budget:20 hrs (c) Search budget:40 hrs (d) Search budget:80 hrs

Figure 9: Search efficiency under time constraints. These results are based on NasBench201 with carbon trace showing in fig. 2, and we ran each method seven times.

Table 5: Search efficiency under carbon emission constraints in terms of Hypervolume. We use the transformer-based carbon predictor in sec. 3.5.2 to forecast the carbon trace and use the actual carbon trace as the baseline. We ran each method ten times and made the average.

Carbon Constrain	**CO2 Cost: 5000g**	**CO2 Cost: 10000g**	**CO2 Cost: 30000g**	**CO2 Cost: 50000g**
Prediction	3724.84	3774.21	3891.70	3966.70
Actual	3742.36	3796.93	3898.43	3971.16

F.2 CE-NAS framework with Time Budget

Our framework also supports neural architecture search (NAS) within a specified time budget, in addition to the option of a carbon budget. We adapt the time budget to replace the carbon budget in the state and reward functions of reinforcement learning. Figure 9 presents the results of our Carbon-Efficient NAS (CE-NAS) under various time budgets. As illustrated, CE-NAS significantly outperforms both heuristic and one-shot methods in terms of hypervolume across different time budgets. While there is a minor decline in performance compared to vanilla NAS as measured by hypervolume, it is important to note that the carbon cost of our CE-NAS is on par with that of the heuristic method. This represents a substantial reduction compared to vanilla NAS. For instance, as depicted in Figure 9(d), vanilla NAS incurs three times the carbon cost of CE-NAS but only achieves a marginal improvement in hypervolume.

F.3 CE-NAS framework with actual carbon trace

As detailed in Section 3.5.2, we implemented a transformer-based carbon predictor to forecast the carbon intensity for the upcoming hour, integrating this predicted value into our framework. The accuracy of this forecast is demonstrated in Fig.2. In the same section, we compare the performance of NAS searches using both the predicted carbon intensity and the actual carbon intensity. Table5 displays the results of our system operating under various carbon budget constraints with both predicted and actual carbon intensities. The data in this table indicates that, across different carbon budgets, employing the predicted carbon intensity trace yields results that are only marginally less effective than using the actual carbon trace, as measured by hypervolume.

Table 6: Search efficiency under carbon emission constraints in terms of Hypervolume. We use the continuous action space of the reinforcement learning method introduced in sec. 3.5.1. We ran each method ten times and made the average.

RL Action Space	**CO2 Cost: 5000g**	**CO2 Cost: 10000g**	**CO2 Cost: 30000g**	**CO2 Cost: 50000g**
Discrete	3724.84	3774.21	3891.70	3966.70
Continuous	3645.21	3748.83	3853.86	3920.47

https://doi.org/10.52202/079017-2628

F.4 CE-NAS framework with continuous RL Action Space

Recall that our RL design includes both a version with a discrete action space and another with a continuous action space. We compare their performance in Table 6 and observe that the two versions deliver comparable performance, with the continuous version performing slightly worse, experiencing a degradation within 3%. Such degradation can be attributed to that the continuous version complicates the action space and increases the learning difficulty. Despite this, we anticipate that the continuous version will outperform its discrete counterpart as the number of available GPUs grows, owing to its more fine-grained GPU allocation decision granularity that gives it the potential to generating better-optimized strategies. We leave the exploration of how GPU cluster sizes impact the relative performance of the two version for future study.

NeurIPS Paper Checklist

1. **Claims**

   Question: Do the main claims made in the abstract and introduction accurately reflect the paper's contributions and scope?

   Answer: [Yes]

   Justification: sec. 1

   Guidelines:

   - The answer NA means that the abstract and introduction do not include the claims made in the paper.
   - The abstract and/or introduction should clearly state the claims made, including the contributions made in the paper and important assumptions and limitations. A No or NA answer to this question will not be perceived well by the reviewers.
   - The claims made should match theoretical and experimental results, and reflect how much the results can be expected to generalize to other settings.
   - It is fine to include aspirational goals as motivation as long as it is clear that these goals are not attained by the paper.

2. **Limitations**

   Question: Does the paper discuss the limitations of the work performed by the authors?

   Answer: [Yes]

   Justification: sec. 4

   Guidelines:

   - The answer NA means that the paper has no limitation while the answer No means that the paper has limitations, but those are not discussed in the paper.
   - The authors are encouraged to create a separate "Limitations" section in their paper.
   - The paper should point out any strong assumptions and how robust the results are to violations of these assumptions (e.g., independence assumptions, noiseless settings, model well-specification, asymptotic approximations only holding locally). The authors should reflect on how these assumptions might be violated in practice and what the implications would be.
   - The authors should reflect on the scope of the claims made, e.g., if the approach was only tested on a few datasets or with a few runs. In general, empirical results often depend on implicit assumptions, which should be articulated.
   - The authors should reflect on the factors that influence the performance of the approach. For example, a facial recognition algorithm may perform poorly when image resolution is low or images are taken in low lighting. Or a speech-to-text system might not be used reliably to provide closed captions for online lectures because it fails to handle technical jargon.
   - The authors should discuss the computational efficiency of the proposed algorithms and how they scale with dataset size.
   - If applicable, the authors should discuss possible limitations of their approach to address problems of privacy and fairness.
   - While the authors might fear that complete honesty about limitations might be used by reviewers as grounds for rejection, a worse outcome might be that reviewers discover limitations that aren't acknowledged in the paper. The authors should use their best judgment and recognize that individual actions in favor of transparency play an important role in developing norms that preserve the integrity of the community. Reviewers will be specifically instructed to not penalize honesty concerning limitations.

3. **Theory Assumptions and Proofs**

   Question: For each theoretical result, does the paper provide the full set of assumptions and a complete (and correct) proof?

   Answer: [NA] .

https://doi.org/10.52202/079017-2628

Justification:

Guidelines:

- The answer NA means that the paper does not include theoretical results.
- All the theorems, formulas, and proofs in the paper should be numbered and cross-referenced.
- All assumptions should be clearly stated or referenced in the statement of any theorems.
- The proofs can either appear in the main paper or the supplemental material, but if they appear in the supplemental material, the authors are encouraged to provide a short proof sketch to provide intuition.
- Inversely, any informal proof provided in the core of the paper should be complemented by formal proofs provided in appendix or supplemental material.
- Theorems and Lemmas that the proof relies upon should be properly referenced.

4. **Experimental Result Reproducibility**

   Question: Does the paper fully disclose all the information needed to reproduce the main experimental results of the paper to the extent that it affects the main claims and/or conclusions of the paper (regardless of whether the code and data are provided or not)?

   Answer: [Yes]

   Justification: See supplemental material.

   Guidelines:

   - The answer NA means that the paper does not include experiments.
   - If the paper includes experiments, a No answer to this question will not be perceived well by the reviewers: Making the paper reproducible is important, regardless of whether the code and data are provided or not.
   - If the contribution is a dataset and/or model, the authors should describe the steps taken to make their results reproducible or verifiable.
   - Depending on the contribution, reproducibility can be accomplished in various ways. For example, if the contribution is a novel architecture, describing the architecture fully might suffice, or if the contribution is a specific model and empirical evaluation, it may be necessary to either make it possible for others to replicate the model with the same dataset, or provide access to the model. In general. releasing code and data is often one good way to accomplish this, but reproducibility can also be provided via detailed instructions for how to replicate the results, access to a hosted model (e.g., in the case of a large language model), releasing of a model checkpoint, or other means that are appropriate to the research performed.
   - While NeurIPS does not require releasing code, the conference does require all submissions to provide some reasonable avenue for reproducibility, which may depend on the nature of the contribution. For example
     (a) If the contribution is primarily a new algorithm, the paper should make it clear how to reproduce that algorithm.
     (b) If the contribution is primarily a new model architecture, the paper should describe the architecture clearly and fully.
     (c) If the contribution is a new model (e.g., a large language model), then there should either be a way to access this model for reproducing the results or a way to reproduce the model (e.g., with an open-source dataset or instructions for how to construct the dataset).
     (d) We recognize that reproducibility may be tricky in some cases, in which case authors are welcome to describe the particular way they provide for reproducibility. In the case of closed-source models, it may be that access to the model is limited in some way (e.g., to registered users), but it should be possible for other researchers to have some path to reproducing or verifying the results.

5. **Open access to data and code**

   Question: Does the paper provide open access to the data and code, with sufficient instructions to faithfully reproduce the main experimental results, as described in supplemental material?

Answer: [Yes]

Justification: See supplemental material.

Guidelines:

- The answer NA means that paper does not include experiments requiring code.
- Please see the NeurIPS code and data submission guidelines (`https://nips.cc/public/guides/CodeSubmissionPolicy`) for more details.
- While we encourage the release of code and data, we understand that this might not be possible, so "No" is an acceptable answer. Papers cannot be rejected simply for not including code, unless this is central to the contribution (e.g., for a new open-source benchmark).
- The instructions should contain the exact command and environment needed to run to reproduce the results. See the NeurIPS code and data submission guidelines (`https://nips.cc/public/guides/CodeSubmissionPolicy`) for more details.
- The authors should provide instructions on data access and preparation, including how to access the raw data, preprocessed data, intermediate data, and generated data, etc.
- The authors should provide scripts to reproduce all experimental results for the new proposed method and baselines. If only a subset of experiments are reproducible, they should state which ones are omitted from the script and why.
- At submission time, to preserve anonymity, the authors should release anonymized versions (if applicable).
- Providing as much information as possible in supplemental material (appended to the paper) is recommended, but including URLs to data and code is permitted.

6. **Experimental Setting/Details**

   Question: Does the paper specify all the training and test details (e.g., data splits, hyperparameters, how they were chosen, type of optimizer, etc.) necessary to understand the results?

   Answer: [Yes]

   Justification: Appendix. E

   Guidelines:

   - The answer NA means that the paper does not include experiments.
   - The experimental setting should be presented in the core of the paper to a level of detail that is necessary to appreciate the results and make sense of them.
   - The full details can be provided either with the code, in appendix, or as supplemental material.

7. **Experiment Statistical Significance**

   Question: Does the paper report error bars suitably and correctly defined or other appropriate information about the statistical significance of the experiments?

   Answer: [Yes]

   Justification: See Appendix. E and Sec. 4

   Guidelines:

   - The answer NA means that the paper does not include experiments.
   - The authors should answer "Yes" if the results are accompanied by error bars, confidence intervals, or statistical significance tests, at least for the experiments that support the main claims of the paper.
   - The factors of variability that the error bars are capturing should be clearly stated (for example, train/test split, initialization, random drawing of some parameter, or overall run with given experimental conditions).
   - The method for calculating the error bars should be explained (closed form formula, call to a library function, bootstrap, etc.)
   - The assumptions made should be given (e.g., Normally distributed errors).
   - It should be clear whether the error bar is the standard deviation or the standard error of the mean.

https://doi.org/10.52202/079017-2628

- It is OK to report 1-sigma error bars, but one should state it. The authors should preferably report a 2-sigma error bar than state that they have a 96% CI, if the hypothesis of Normality of errors is not verified.
- For asymmetric distributions, the authors should be careful not to show in tables or figures symmetric error bars that would yield results that are out of range (e.g. negative error rates).
- If error bars are reported in tables or plots, The authors should explain in the text how they were calculated and reference the corresponding figures or tables in the text.

8. **Experiments Compute Resources**

   Question: For each experiment, does the paper provide sufficient information on the computer resources (type of compute workers, memory, time of execution) needed to reproduce the experiments?

   Answer: [Yes]

   Justification: See Appendix. E

   Guidelines:

   - The answer NA means that the paper does not include experiments.
   - The paper should indicate the type of compute workers CPU or GPU, internal cluster, or cloud provider, including relevant memory and storage.
   - The paper should provide the amount of compute required for each of the individual experimental runs as well as estimate the total compute.
   - The paper should disclose whether the full research project required more compute than the experiments reported in the paper (e.g., preliminary or failed experiments that didn't make it into the paper).

9. **Code Of Ethics**

   Question: Does the research conducted in the paper conform, in every respect, with the NeurIPS Code of Ethics `https://neurips.cc/public/EthicsGuidelines`?

   Answer: [Yes]

   Justification:

   Guidelines:

   - The answer NA means that the authors have not reviewed the NeurIPS Code of Ethics.
   - If the authors answer No, they should explain the special circumstances that require a deviation from the Code of Ethics.
   - The authors should make sure to preserve anonymity (e.g., if there is a special consideration due to laws or regulations in their jurisdiction).

10. **Broader Impacts**

    Question: Does the paper discuss both potential positive societal impacts and negative societal impacts of the work performed?

    Answer: [Yes]

    Justification:

    Guidelines:

    - The answer NA means that there is no societal impact of the work performed.
    - If the authors answer NA or No, they should explain why their work has no societal impact or why the paper does not address societal impact.
    - Examples of negative societal impacts include potential malicious or unintended uses (e.g., disinformation, generating fake profiles, surveillance), fairness considerations (e.g., deployment of technologies that could make decisions that unfairly impact specific groups), privacy considerations, and security considerations.
    - The conference expects that many papers will be foundational research and not tied to particular applications, let alone deployments. However, if there is a direct path to any negative applications, the authors should point it out. For example, it is legitimate to point out that an improvement in the quality of generative models could be used to

generate deepfakes for disinformation. On the other hand, it is not needed to point out that a generic algorithm for optimizing neural networks could enable people to train models that generate Deepfakes faster.

- The authors should consider possible harms that could arise when the technology is being used as intended and functioning correctly, harms that could arise when the technology is being used as intended but gives incorrect results, and harms following from (intentional or unintentional) misuse of the technology.
- If there are negative societal impacts, the authors could also discuss possible mitigation strategies (e.g., gated release of models, providing defenses in addition to attacks, mechanisms for monitoring misuse, mechanisms to monitor how a system learns from feedback over time, improving the efficiency and accessibility of ML).

11. **Safeguards**

    Question: Does the paper describe safeguards that have been put in place for responsible release of data or models that have a high risk for misuse (e.g., pretrained language models, image generators, or scraped datasets)?

    Answer: [NA] .

    Justification:

    Guidelines:

    - The answer NA means that the paper poses no such risks.
    - Released models that have a high risk for misuse or dual-use should be released with necessary safeguards to allow for controlled use of the model, for example by requiring that users adhere to usage guidelines or restrictions to access the model or implementing safety filters.
    - Datasets that have been scraped from the Internet could pose safety risks. The authors should describe how they avoided releasing unsafe images.
    - We recognize that providing effective safeguards is challenging, and many papers do not require this, but we encourage authors to take this into account and make a best faith effort.

12. **Licenses for existing assets**

    Question: Are the creators or original owners of assets (e.g., code, data, models), used in the paper, properly credited and are the license and terms of use explicitly mentioned and properly respected?

    Answer: [Yes]

    Justification: See [1].

    Guidelines:

    - The answer NA means that the paper does not use existing assets.
    - The authors should cite the original paper that produced the code package or dataset.
    - The authors should state which version of the asset is used and, if possible, include a URL.
    - The name of the license (e.g., CC-BY 4.0) should be included for each asset.
    - For scraped data from a particular source (e.g., website), the copyright and terms of service of that source should be provided.
    - If assets are released, the license, copyright information, and terms of use in the package should be provided. For popular datasets, `paperswithcode.com/datasets` has curated licenses for some datasets. Their licensing guide can help determine the license of a dataset.
    - For existing datasets that are re-packaged, both the original license and the license of the derived asset (if it has changed) should be provided.
    - If this information is not available online, the authors are encouraged to reach out to the asset's creators.

13. **New Assets**

    Question: Are new assets introduced in the paper well documented and is the documentation provided alongside the assets?

https://doi.org/10.52202/079017-2628

Answer: [Yes]

Justification: See our supplementary material.

Guidelines:

- The answer NA means that the paper does not release new assets.
- Researchers should communicate the details of the dataset/code/model as part of their submissions via structured templates. This includes details about training, license, limitations, etc.
- The paper should discuss whether and how consent was obtained from people whose asset is used.
- At submission time, remember to anonymize your assets (if applicable). You can either create an anonymized URL or include an anonymized zip file.

14. **Crowdsourcing and Research with Human Subjects**

Question: For crowdsourcing experiments and research with human subjects, does the paper include the full text of instructions given to participants and screenshots, if applicable, as well as details about compensation (if any)?

Answer: [NA] .

Justification:

Guidelines:

- The answer NA means that the paper does not involve crowdsourcing nor research with human subjects.
- Including this information in the supplemental material is fine, but if the main contribution of the paper involves human subjects, then as much detail as possible should be included in the main paper.
- According to the NeurIPS Code of Ethics, workers involved in data collection, curation, or other labor should be paid at least the minimum wage in the country of the data collector.

15. **Institutional Review Board (IRB) Approvals or Equivalent for Research with Human Subjects**

Question: Does the paper describe potential risks incurred by study participants, whether such risks were disclosed to the subjects, and whether Institutional Review Board (IRB) approvals (or an equivalent approval/review based on the requirements of your country or institution) were obtained?

Answer: [NA] .

Justification:

Guidelines:

- The answer NA means that the paper does not involve crowdsourcing nor research with human subjects.
- Depending on the country in which research is conducted, IRB approval (or equivalent) may be required for any human subjects research. If you obtained IRB approval, you should clearly state this in the paper.
- We recognize that the procedures for this may vary significantly between institutions and locations, and we expect authors to adhere to the NeurIPS Code of Ethics and the guidelines for their institution.
- For initial submissions, do not include any information that would break anonymity (if applicable), such as the institution conducting the review.